CDF/DOC/JET/CDFR/7930
March 24, 2006

First Observation of Exclusive Electron Pairs in Hadron-Hadron Collisions

Andrew Hamilton[1)1], Michael Albrow[2)], Bryan Caron[1)], Beate Heinemann[3)], and Jim Pinfold[1)]

1) University of Alberta 2) Fermi National Accelerator Laboratory
3) University of Liverpool

Abstract

We present the observation of 16 exclusive e^+e^- events on top of a background of estimate of $2.1^{+0.6}_{-0.3}$. Each event has an e^+e^- pair (both with $p_T > 5$ GeV) and *nothing else* observable in the CDF detector. The measured cross section is $1.6\ ^{+0.5}_{-0.3}$(stat) ± 0.3(sys) pb, while the predicted cross section is 1.711 ± 0.008 pb. The events are consistent in cross section and properties with with $p\bar{p} \to p + e^+e^- + \bar{p}$ through two photon exchange ($\gamma\gamma \to e^+e^-$). Two photon collisions have previously been studied in e^+e^- collisions at LEP and elsewhere, but this is the first observation in hadron-hadron collisions.

Contents

[1]Ph.D. thesis

1 Introduction

Photon-photon collisions have been much studied in e^+e^- collisons at PETRA [1], TRISTAN [2] and LEP [3, 4, 5], the two photons being radiated off the incoming electrons, which emerge in the forward direction with some momentum loss, where they may be tagged [6]. At LEP-II ($\sqrt{s} = 200$ GeV) the cross-section for $e^+e^- \to e^+e^-$ hadrons, with $W_{\gamma\gamma} > 5$ GeV is 12 nb, 160 times higher than the annihilation reaction $e^+e^- \to \gamma/Z \to q\bar{q}(\gamma)$. The ratio rises with $\sqrt{s}$, so at the ILC it will be much higher.

Photon-photon collisions have not previously been observed in hadron-hadron collisions, having a very small cross section ($\sim$ pb) compared to the strong interaction cross section, $\sigma_{tot} \approx 80$ mb and $\sigma_{inel} \approx 60$ mb. The most promising channels are $\gamma\gamma \to e^+e^-$ and $\gamma\gamma \to \mu^+\mu^-$, with the p and $\bar{p}$ coherently scattered, thus $p\bar{p} \to p + e^+e^-(\mu^+\mu^-) + \bar{p}$; no other particles are produced, i.e. it is an *exclusive* reaction, see Figure 1.

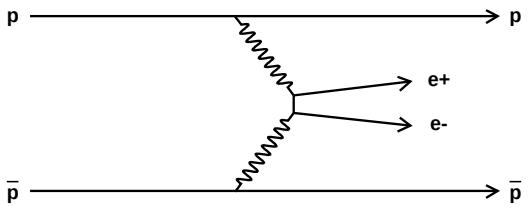

Figure 1: Feynman diagram of exclusive e^+e^- via two photon exchange.

The main process for producing lepton pairs in hadron-hadron collisions is Drell-Yan, $q\bar{q} \to l^+l^-$. Removal of a color triplet from the protons results in a color dipole which fills rapidity with hadrons, usually with a large multiplicity. The only way that could be avoided is to exchange another color triplet to leave the protons as color singlets, with a very small probability of not dissociating; this cross section is negligible. On the other hand the photon process is (almost[2]) pure QED. The only

[2]In principle one can have pomeron exchange between the protons, in addition to the photon. The correction is small at these large impact parameters because the range of the strong force is $\sim$fermi,

non-fundamental part is the electromagnetic form factor of the proton, which is well known (and in the limit $t \to 0$ becomes 1).

The process in hadron collisions was first discussed in 1972 by Budnev, Ginsburg, Meledin and Serbo [8]. Other papers, mainly considering it as a process for luminosity calibration, are by Shamov and Telnov [9], Piotrzkowski [10], and Caron and Pinfold [11].

Apart from its intrinsic interest, measurement of the process would be another way of calibrating the luminosity monitors of collider experiments. To do this without knowing σ_{inel} one needs to count all events, even in the presence of pile-up. This should be possible with $\mu^+\mu^-$ thanks to three features: (1) the muons are almost exactly back-to-back in azimuth (2) they have almost the same p_T (3) there are no other charged tracks on the $\mu^+\mu^-$ vertex. The first two properties arise because the interaction is highly peripheral (at large distances the strong field has died away leaving the electromagnetic field dominant) and therefore the protons have very small t (i.e. p_T), typical of Coulomb scattering.

Another use of this process as a tool is that from the very accurate measurements of the leptons one knows the momenta of the forward protons. One has:

$$\xi_{1(2)} = \frac{1}{\sqrt{s}} \sum_{i=1,2} p_T(i) e^{-(+)\eta(i)}$$

where ξ is the fractional momentum loss of the protons. This can be used to calibrate the momentum scale of forward proton detectors; indeed for the LHC it seems to be the most promising method. In CDF the roman pots (on the outgoing $\bar{p}$-side) do not have acceptance for low-t and low-ξ and are not used in this analysis.

In the study presented here, the primary motivation was actually to search for a rarer process, namely the exclusive production of two photons, $p\bar{p} \to p + \gamma\gamma + \bar{p}$. By making no track requirements until the last step in the analysis we retain both e^+e^- and $\gamma\gamma$ events. The $\gamma\gamma$ analysis is presented in another note [16]. The measurement of the well known e^+e^- cross section adds confidence to the theoretically less certain $\gamma\gamma$ measurement.

2 Monte Carlo

The LPAIR program [7] is a matrix element Monte Carlo simulation of two photon production of fermion pairs for incoming beams of electrons, positrons, protons, and anti-protons. The code presents a numerically stable program for all collision energies through a reformulation of the basic phase space integrals. This enables easier treatment of discontinuities resulting from the application of experimental cuts with the generator code. LPAIR is written in Fortran-77 and utilizes the VEGAS [17] automatic integration routine.

Three categories of two photon collisions from the incoming proton anti-proton beams of the Tevatron can be simulated with LPAIR. The elastic-elastic process is the generator configuration used to simulate the expected signal for this analysis. The elastic-inelastic and inelastic-inelastic configurations are used to help estimate the background.

1. elastic-elastic $p\overline{p} \to p + l^+l^- + \overline{p}$

while EM is unlimited

2. elastic-inelastic $p\overline{p} \to p + l^+l^- + X$ and $p\overline{p} \to X + l^+l^- + \overline{p}$
3. inelastic-inelastic $p\overline{p} \to X + l^+l^- + X$

The cross section for elastic-elastic production of electron pairs with $p_T(e) > 5.0$ GeV, $|\eta| < 2.0$ at the Tevatron, $\sqrt{s} = 1960$ GeV, is predicted by LPAIR Monte Carlo to be $\sigma_{peep} = 1.711 \pm 0.008$ pb [7].

3 Event Selection

Selecting potentially interesting events from the 1.7 million bunch crossings per second is done with a trigger to write the events to tape, and sequence of offline cuts to select interesting events from those on tape. The offline cuts include electron ID (which identify electrons in the detector), exclusivity cuts (which check that there is no other observable particles in the detector), and cosmic cuts (which eliminate cosmic rays).

3.1 Trigger and Good Run List

A trigger, with path name DIFF_DIPHOTON, is used for this analysis. It was implemented to search for exclusive production of two photons [16]. The details of the trigger cuts are shown in Table 1. The trigger rate is very low and peaks at an instantaneous luminosity of about 20E30cm^{-2}s^{-1}, as shown in Figure 2. The peak in the trigger rate at 20E30cm^{-2}s^{-1}is expected [14] because multiple interactions spoil the rapidity gap requirement.

The trigger has been in since December 7, 2004 in the low luminosity trigger tables "PHYSICS_3_$\star$".[3]. The data used in the current analysis is the "gdif0h" dataset, which corresponds to runs 190697 to 206989 taken between December 7 2004 and November 9 2005. The dataset was produced with the CDFSOFT2 6.1.1 version of production and ntuplized into the dev_243 Stntuple with CDFSOFT2 6.1.2. The ntuplized dataset contains xxx events that passed the DIFF_DIPHOTON trigger.

A good run list is applied to the dataset to eliminate runs in which a detector component was not functioning properly. The good run list used is a subset of the DQM version 11 list in which runs that were bad for SMX (Shower Max), MP (Miniplug), BSC (Beam Shower Counter) were removed, as well as runs that used the high luminosity trigger tables and runs greater than 206989. The total integrated luminosity for these runs corresponds to 522 ± 32 pb^{-1}. The systematic uncertainty applied is 6% for the default CDF luminosity calibration.

3.2 Electron ID Cuts

The first step in the offline event selection is selecting electron candidates from the EM objects in the triggered events. Since this analysis is being done in parallel with the search for exclusive two photon production, the initial cuts will pass both electrons and photons. The only measurable difference between photons and electrons in the CDF detector is the electron track, so the track requirement will be applied last.

The ID cuts applied are shown in Table 2. They are based on the standard photon cuts recommended by the photon group. An EM object that passes the cuts in Table 2

[3]The trigger was in for a short time from August 9-23 2004, runs 186081-186598 corresponding to 8.8 pb^{-1}which is not used in this analysis.

DIFF_DIPHOTON Trigger Details	
Level 1: L1_TWO_GAP_&_EM4	East + West BSC Empty, and 1 Plug or Central tower with: (HadEm<0.125) & (Et>4GeV)
Level 2: L2_TWO_EM4	2 EM objects (plug or central) with: (HadEm< 0.125) & (Et>4GeV) & ($0 < |\eta| < 3.6$)
Level 3: L3_DIPHOTON4	2 EM objects (plug or central) with: (Et>4GeV) & (Iso<2GeV or IsoRatio<0.1) & (CES $\chi^2 < 20.0$)†

Table 1: Details of DIFF_DIPHOTON trigger cuts. † denotes the cut is central only.

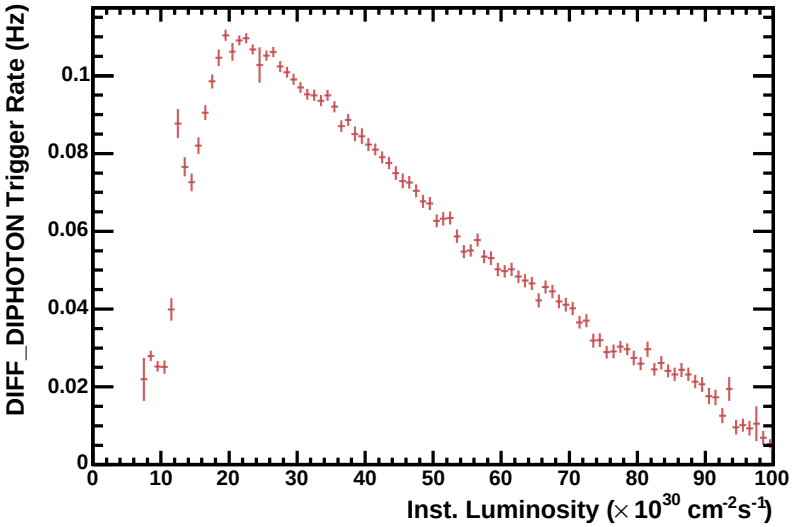

Figure 2: Trigger rate as a function of instantaneous luminosity for the DIFF_DIPHOTON trigger (trigger table PHYSICS_3_0[0-2] bit #37).

Cut	Central	Plug
Energy (GeV)	$E_t > 5.0$	$E_t > 5.0$
Shower Shape	CES χ^2 <20	PES χ^2 <10
Had/Em Ratio	< 0.055 + 0.00045*E	< 0.05

Table 2: Details of electron candidate cuts (energy units are GeV).

will be called an *electron candidate*. The collection of all events with two canadiates will be refered to as the *two-candidate sample*. The standard isolation cuts are not applied in this set of loose cuts because the exclusivity cuts are equivalent to isolation cuts. The exclusivity cuts are explained in Section 3.4.

3.3 Cosmic Cut

In order to remove cosmic rays from the data sample, the EM timing of each electron must be less than 10 ns, the difference between the EM timing of the two electrons is required to be less than 5 ns, and the electrons are required to be separated by more than 90deg in ϕ. The efficiency and background of this cut is discussed in Sections 4.3 and 5.2. While more cuts on other variables could be applied, we choose to use only the EM timing and $\Delta\phi$ cuts because it can be used for both photon and electron samples. xxx of the xxx two candidate events pass this cosmic cut.

3.4 Exclusivity Cuts

In order to determine if the event was exclusive, one must determine that there was nothing (other than the two EM objects) in the detector. In order to do that, you must know what "nothing" looks like in the detector. To accomplish this, two samples of events were made from zerobias data, *interaction* and *non-interaction*. Events with no tracks (above the default CDF track of 200 MeV/c), no hits in the CLC (a hit defined as >150 ADC counts), and no muon stubs, were put into the non-interaction sample, all others were put into the interaction sample. In the remainder of this section these samples will be used to motivate the exclusivity cuts on the Beam Shower Counter (BSC) and calorimeters. Note that the no track, CLC, and muon cuts are not being applied to the exclusive electron sample, they are only being use to help define appropriate calorimeter cuts that will be applied to the signal sample.

Figure 3 shows the maximum number of ADC counts in any of the BSC-1 PMTs for the interaction and non-interaction samples (one entry per event). It shows that 300 ADC counts distinguishes between an interaction and no interaction in BSC-1. 300 ADC counts is therefore the exclusivity cut on the BSC-1, meaning that an event must have all BSC-1 channels less than 300 counts to be defined as exclusive. Since the physical origin of the distribution in the 300 to 1000 counts region is not completely understood, the more conservative cut of 300 counts was chosen. Figures 4 and 5 show the corresponding plots for BSC-2 and BSC-3. A cut of 400 counts is choosen for BSC-3 because the pedestal is wider.

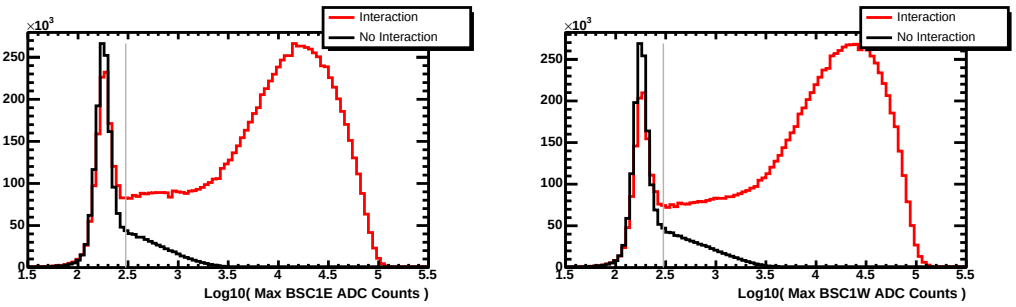

Figure 3: Log10(ADC counts - pedestal) in BSC-1 for interaction and non-interaction samples, the line shows the cut at 300 counts. Left plots are east, right plots are west.

The calorimeters are divided into five regions; mini-plug region (towers 22 to 25 $3.6 < |\eta| < 5.2$), the forward-plug region (towers 18 to 21 $2.11 < |\eta| < 3.64$), the mid-plug region (towers 12 to 17 $1.32 < |\eta| < 2.11$), and the end-wall region (towers

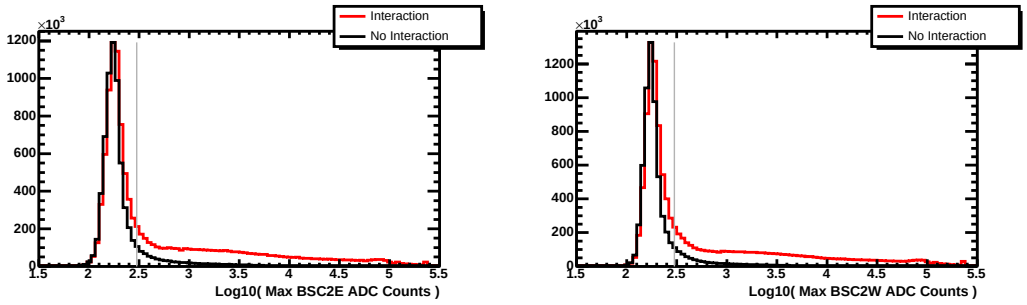

Figure 4: Log10(ADC counts - pedestal) in BSC-2 for interaction and non-interaction samples, the line shows the cut at 300 counts. Left plots are east, right plots are west.

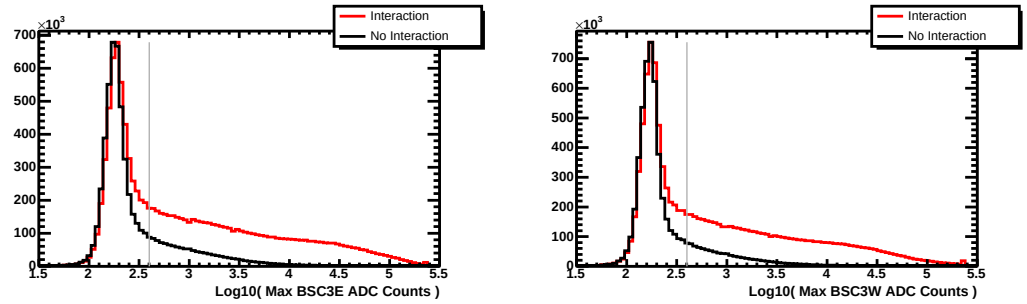

Figure 5: Log10(ADC counts - pedestal) in BSC-3 for interaction and non-interaction samples, the line shows the cut at 400 counts. Left plots are east, right plots are west.

6 to 11 $0.66 < |\eta| < 1.32$), and the central region (towers 0 to 5 $0.00 < |\eta| < 0.66$). Figures 6 to 11 show the highest E_T tower for the five regions in the interaction and non-interaction samples. The central and end-wall regions are divided into EM tower and HAD tower cuts due to the large difference in the noise levels of the two sections[4]. These plots motivate the cuts shown in Table 3.

The exclusivity cuts are applied to all towers in two-candidate events except for the electron towers. An electron tower is defined as any tower in the CdfEmObject's TowerLinkList plus any towers within $\Delta itow < 1.5$, where $\Delta itow \equiv \sqrt{\Delta ieta^2 + \Delta iphi^2}$. The number of two-candidate events that pass each cut (in sequence from BSC to Central) is shown in Table 4.

[4]The CalData block has a default PMT spike killer for towers greater than 500 MeV, a spike killer routine below 500 MeV was developed by Angela Wyatt 7.2 and is applied to all towers.

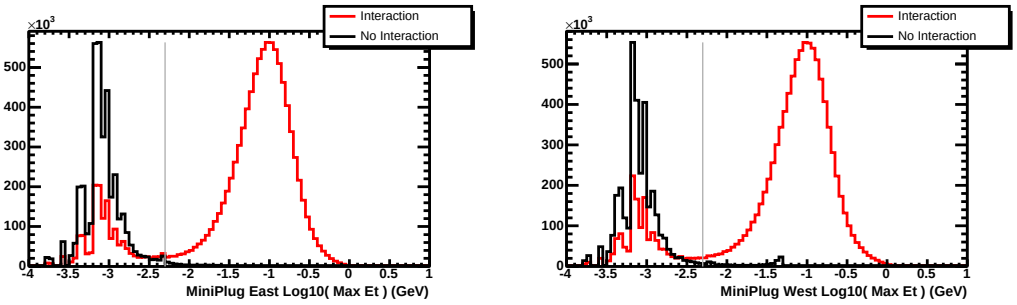

Figure 6: Log10(Max Et) hit in mini-plug for interaction and non-interaction samples, the line shows the 5 MeV cut. Left plots are east, right plots are west.

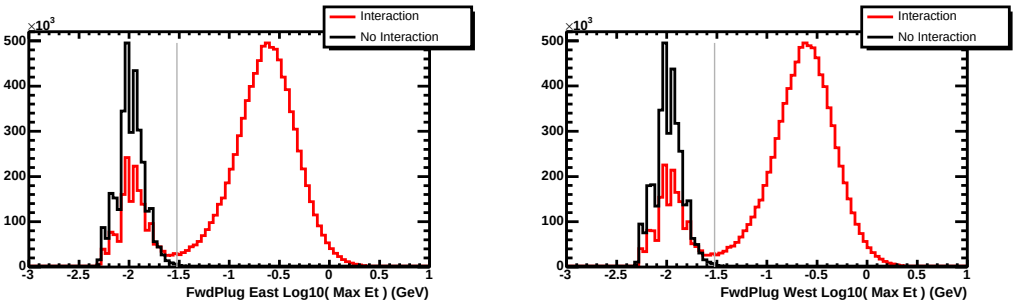

Figure 7: Log10(Max Et) tower in the forward-plug region for interaction and non-interaction samples, the line shows the 30 MeV cut. Left is east, right is west.

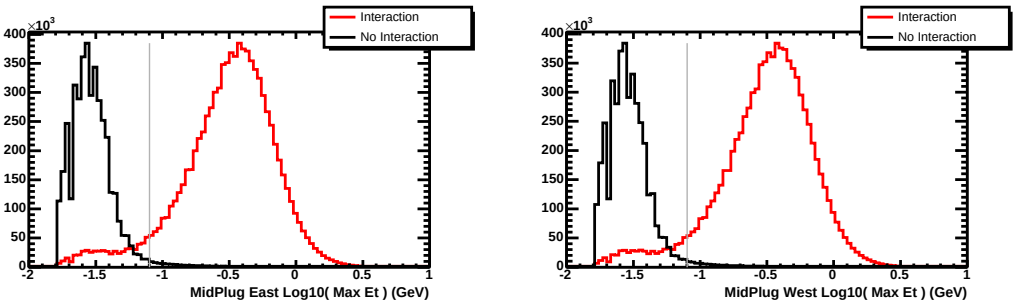

Figure 8: Log10(Max Et) tower in the mid-plug region for interaction and non-interaction samples, the line shows the 80 MeV cut. Left is east, right is west.

3.5 Track Cut

As shown in Table 4, 27 events from the two-candidate sample pass the exclusive cuts. To distingush the electrons from photons, each electron candidate is required to have

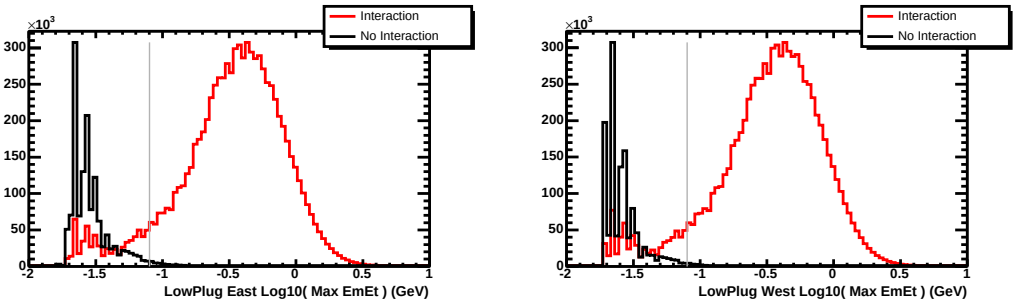

Figure 9: Log10(Max Et) EM tower in the end-wall region for interaction and non-interaction samples, the line shows the 80 MeV cut. Left is east, right is west.

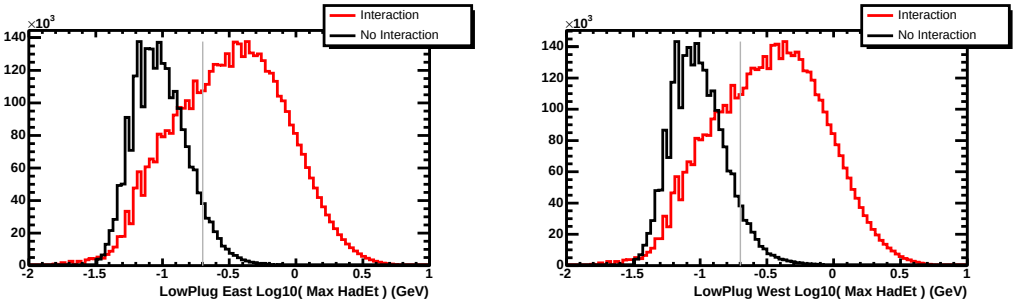

Figure 10: Log10(Max Et) HAD tower in the end-wall region for interaction and non-interaction samples, the line shows the 200 MeV cut. Left is east, right is west.

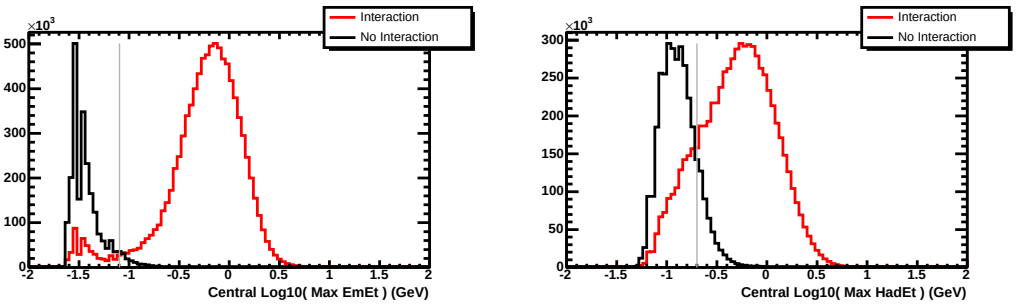

Figure 11: Log10(Max Et) tower in the central region for interaction and non-interaction samples, the line shows the 80 MeV and 200 MeV cuts for EM and Hadronic sections. Left is EM, right is Hadronic.

a single track with p_T >1 GeV. 16 events pass this cut. These events are called the *signal sample*, and are discussed in the following section.

Region	Towers	Eta Range	Cut
BSC-3	n/a	$6.7 < \|\eta\| < 7.4$	<400 ADC counts
BSC-2	n/a	$6.4 < \|\eta\| < 7.1$	<300 ADC counts
BSC-1	n/a	$5.4 < \|\eta\| < 5.9$	<300 ADC counts
MiniPlug	22 to 25	$3.6 < \|\eta\| < 5.2$	$E_T < 5$ MeV
Forward Plug	18 to 21	$2.11 < \|\eta\| < 3.64$	$E_T < 30$ MeV
Mid Plug	12 to 17	$1.32 < \|\eta\| < 2.11)$	$E_T < 80$ MeV
End Wall	6 to 11	$0.66 < \|\eta\| < 1.32$	EM $E_T < 80$ MeV, HAD $E_T < 200$ MeV
Central	0 to 5	$0.00 < \|\eta\| < 0.66$	EM $E_T < 80$ MeV, HAD $E_T < 200$ MeV

Table 3: Summary of exclusivity cuts

Sample	Number of Events
Two-candidate events (no cosmics)	xxx
Pass All BSC	12433
Pass MiniPlug	489
Pass FwdPlug	95
Pass MidPlug	68
Pass EndWall	33
Pass Central	27

Table 4: Number of two-candidate events remaining after each exclusive cut

3.6 Signal Sample

The signal sample of 16 events is given in Appendix 7.3 and compared to the LPAIR Monte Carlo in Figures 12 to 16. They show that there is agreement between the data and MC within the statistics of the sample. Figures 17 shows an event display of a typical signal event; run 195762, event 3788.

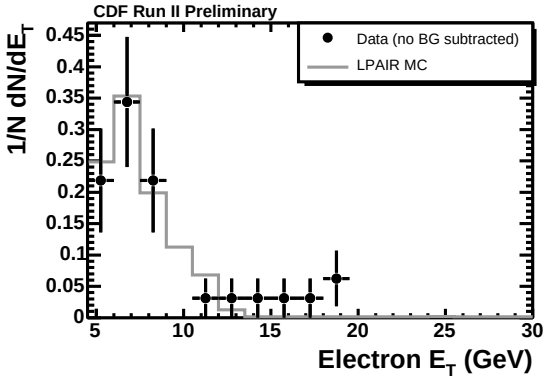

Figure 12: E_T of electrons in signal sample (points) compared to LPAIR MC (line)

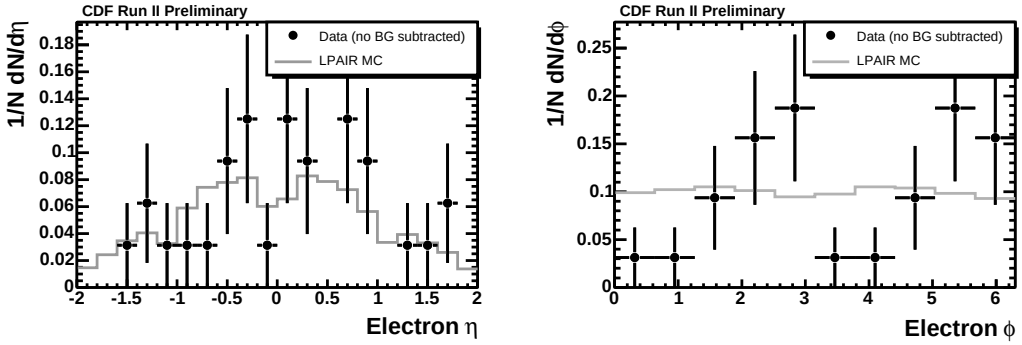

Figure 13: eta (left) and phi (right) of electrons in signal sample (points) compared to LPAIR MC (line)

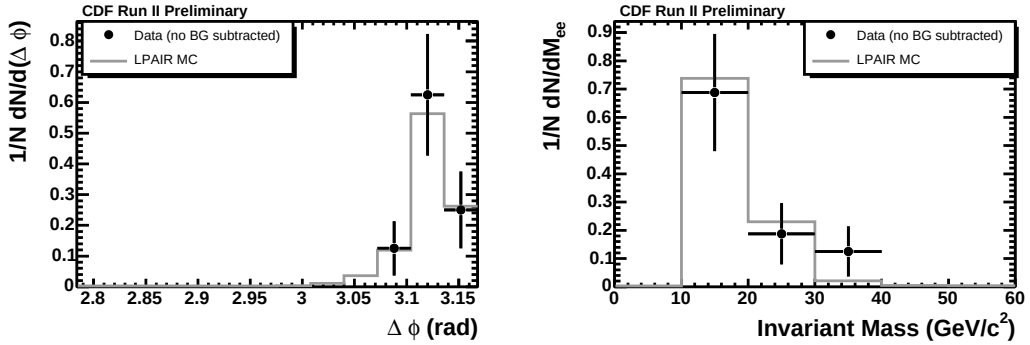

Figure 14: Delta ϕ (left) and invariant mass (right) of ee pairs in signal sample (points) compared to LPAIR MC (line)

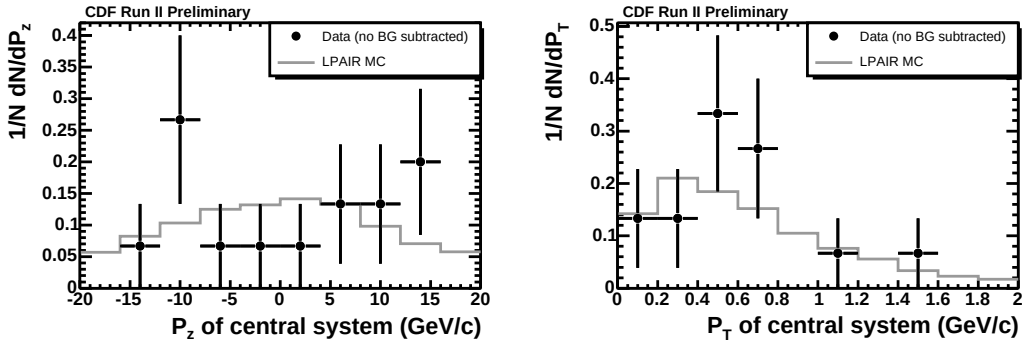

Figure 15: p_z and p_t of ee pairs in signal sample (points) compared to LPAIR MC (line)

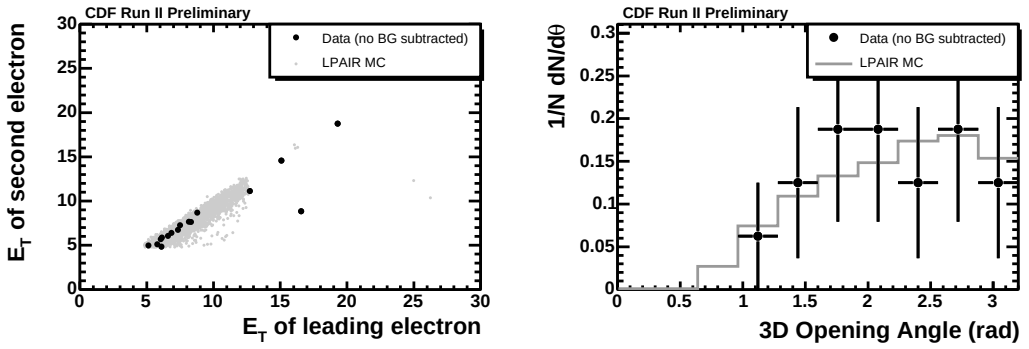

Figure 16: E_T of leading electron vs E_T of second electron (left) and 3-D opening angle of ee pairs in signal sample (points) compared to LPAIR MC (line) (right)

4 Efficiencies

There are four efficiencies to be folded into the cross section calculation:

ε_{ee} the efficiency for identifying the two electrons

ε_{exc} the efficiency of the exclusivity cuts

ε_{fsr} the efficiency for events which undergo some final state radiation

ε_{cos} the efficiency for the cosmic cut

Since an inelastic $p\bar{p}$ interaction on top of an exclusive interaction in a beam crossing will make the exclusive interaction unobservable, ε_{exc} is highly dependent on instantaneous luminosity. Accounting for ε_{exc} in the cross section is done with a quantity called the *effective luminosity*, $\mathscr{L}_{eff}$, which is explained in Section 4.4. The calculation of ε_{ee}, ε_{fsr}, and ε_{cos} are not dependent on instantaneous luminosity. They are shown in Sections 4.1 and 4.2. For clarity, the cross section equation with efficiencies is given

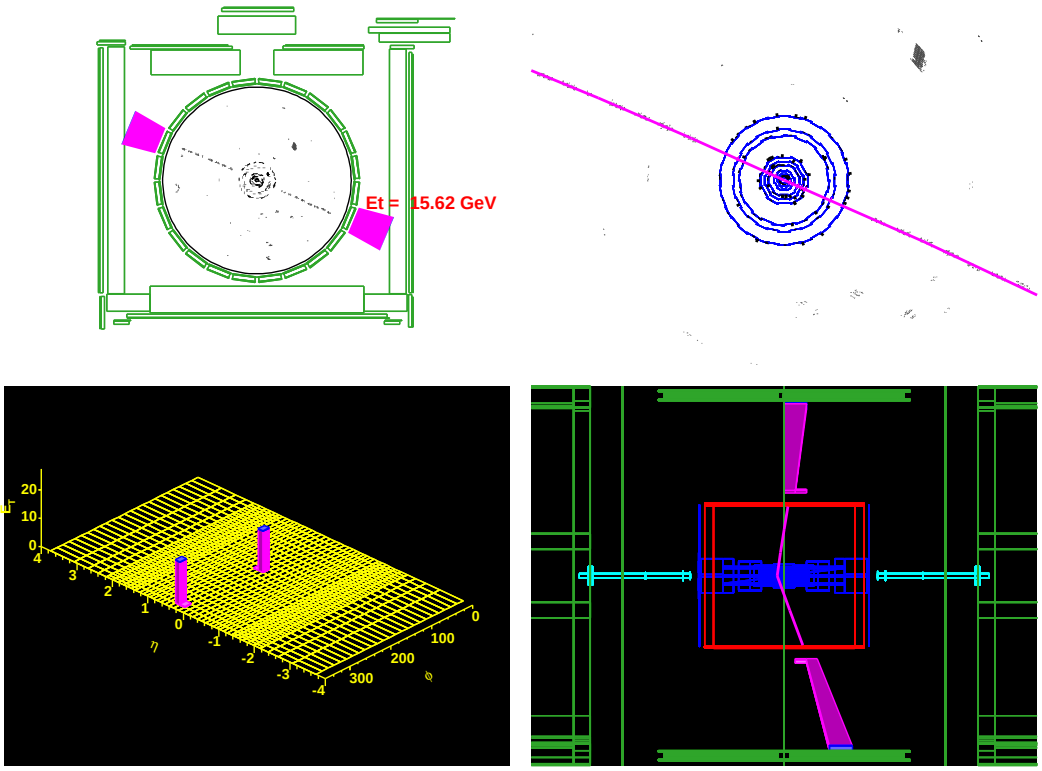

Figure 17: Event display of run 195762 event 3788.

here:

$$\sigma = \frac{N_{signal} - N_{bkgd}}{\varepsilon_{ee}\varepsilon_{fsr}\varepsilon_{cos}\mathscr{L}_{eff}} \tag{1}$$

4.1 Electron Efficiency

The electron efficiency can be broken into four parts; reconstruction efficiency, $\varepsilon_{ee,rec}(E_T)$, trigger efficiency, $\varepsilon_{e,trig}(E_T)$, ID efficiency, $\varepsilon_{e,id}$, and tracking efficiency $\varepsilon_{e,trk}$. The reconstruction and trigger efficiencies are both functions of E_T . The expected signal (from LPAIR Monte Carlo) is a steeply falling function of E_T , so the LPAIR E_T distribution must be taken into account for these efficiencies.

The reconstruction efficiency is denoted with subscript "ee", rather than just "e", to reflect the fact that this efficiency must be calculated per event, rather than per electron, due to the ϕ correlation between the two electrons. This notation will be carried through the note, subscript "ee" meaning per event and subscript "e" meaning per electron. The four parts can be combined to calculate the total electron efficiency, Equation 2.

$$\varepsilon_{ee} = \varepsilon_{ee,rec} \cdot \varepsilon^2_{e,trig} \cdot \ \varepsilon^2_{e,id}\varepsilon^2_{e,trk} \tag{2}$$

Reconstruction Efficiency, $\varepsilon_{ee,rec}$

The electron reconstruction efficiency, $\varepsilon_{e,rec}$, accounts for electrons that do not get identified as electromagnetic objects in the offline data - they have fallen into inactive parts of the detector, like the cracks between the ϕ wedges and the crack at η =0 of the calorimeter. Since the two electrons in the event are highly correlated (back-to-back in dϕ and balanced in E_T), the probability of finding both electrons is not equal to the square of the probability of finding one electron (if one falls into a ϕ crack, the other is more like to fall into a ϕ crack). Therefore, $\varepsilon_{e,rec}$ is calculated using the signal Monte Carlo, LPAIR, on an event-by-event basis. Events generated with LPAIR are put through detector simulation, cdfSim version 5.3.3, and ntuplized with Stntuple dev_242.

Reconstruction efficiency is as defined:

$$\varepsilon_{ee,rec} \equiv \frac{N_{gen+rec}}{N_{gen}} \tag{3}$$

The denominator, N_{gen}, is the number of events generated with both electrons having $|\eta| < 2.0$. The numerator, $N_{gen+rec}$, is the number of events from the denominator that have both reconstructed electrons within $\Delta R < 0.4$[5] of the generated electron. A reconstructed electron is defined as a TStnElectron (CDFEmObject) in the Stntuple's TStnElectronBlock. Using this presciption, the reconstruction efficiency is 0.69±0.02, where the uncertainty is the systematic evaluated by changing the energy scale (E_T cut) by 1%. The choice of 1% is based on Figure 13 of CDFNOTE 7543 [12], showing that the energy scale in CDFSim is accurate to within 1%. Figures 18 and 19 show $\varepsilon_{ee,rec}$ as a function of E_T , η , and ϕ .

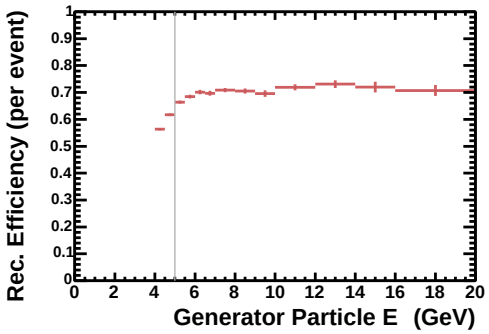

Figure 18: Electron reconstruction efficiency, $\varepsilon_{ee,rec}$, as a function of generator electron E_T .

Electron Trigger Efficiency

The trigger efficiency accounts for those electrons that would get reconstructed and pass all offline criteria, but fail the trigger. The trigger efficiency, ε_{trig}, can be defined

[5] $\Delta R \equiv \sqrt{\Delta\eta^2 + \Delta\phi^2}$

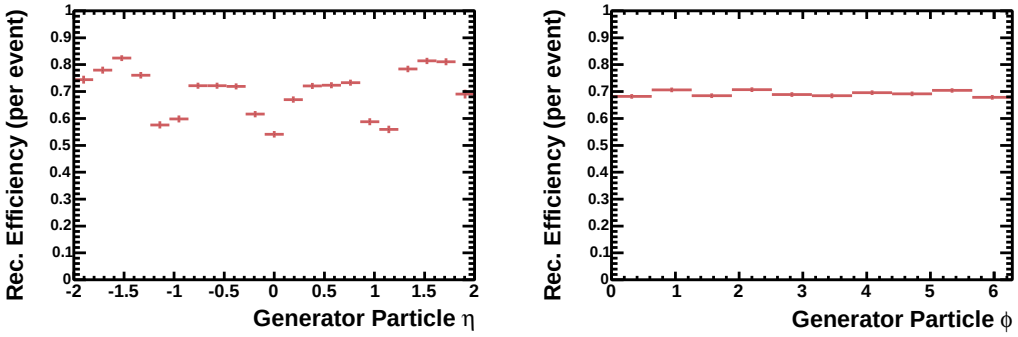

Figure 19: Electron reconstruction efficiency, $\varepsilon_{\gamma,rec}$, as a function of generator electron η and ϕ

as

$$\varepsilon_{e,trig} \equiv \frac{N_{trig+id}}{N_{id}} \tag{4}$$

The denominator, N_{id}, are electrons selected from minbias[6] data as electrons that pass all the ID cuts. Using minbias data gives a sample with no trigger bias. The numerator, $N_{trig+id}$, is found by determining how many of the N_{id} sample would have passed the electron trigger requirements (a match between a trigger and offline electron is defined as having the same seed tower).

To determine whether or not they would pass the trigger requirements we used the TTl2dCluster (from TL2D bank) and TL3Em (from TL3Summary bank) in the Stntuple, to simulate the Level 2 and Level 3 triggers. Level 1 has no effect on the trigger efficiency because any electron which passes the L2 trigger will pass the L1 trigger (L2 has a shoulder energy requirement of 127 GeV, rendering it a 'single-tower' trigger like L1). Table 5 shows the variables and cut values of the simulated trigger requirements (compare to the values in Table 1).

Trigger efficiency as a function of E_T , η , and ϕ are shown in Figures 20 and 21. The trigger efficiency as a function of E_T must be applied to the expected signal sample because the E_T distribution in exclusive events is slightly steeper than that of EMObjects in minbias data. $\varepsilon_{e,trig}$ is calculated from Figure 22 as the total number of LPAIR events times the efficiency (filled histogram) divided by the number of LPAIR events (empty histogram). The efficiency as a function of E_T is also shown on Figure 22. This weighting does not need to be done for the η distribution, since the minbias and expected signal distribution are similar in η . The integrated trigger efficiency is therefore 0.77±0.05, where the systematic uncertainty is evaluated by varying the value of the trigger efficiency (for each bin) by the upper and lower bounds of the efficiency as a function of E_T .

[6]minbias means data taken with the minimum bias trigger, an east-west coincidence of the CLC detectors

TTl2dCluster::EtEmGeV()	>= 4.0 GeV
TTl2dCluster::EtHadGeV()/EtEmGeV()	<= 0.125
|TTl2dCluster::DetEta()|	<= 3.6
TL3Em::CesAvgChi2()	<=20.0
TL3Em::Phet()	>=4.0
TL3Em::Hadem3()	<=0.125
TL3Em::PhoIso4()*	<=2.0
TL3Em::PhoIso4()/Phet()*	<=0.1

Table 5: Cuts made in simulation of trigger, * denotes an OR between the variables. NB TL3Em::CesAvgChi2() had to be corrected due to a bug in production, see Appendix 7.1

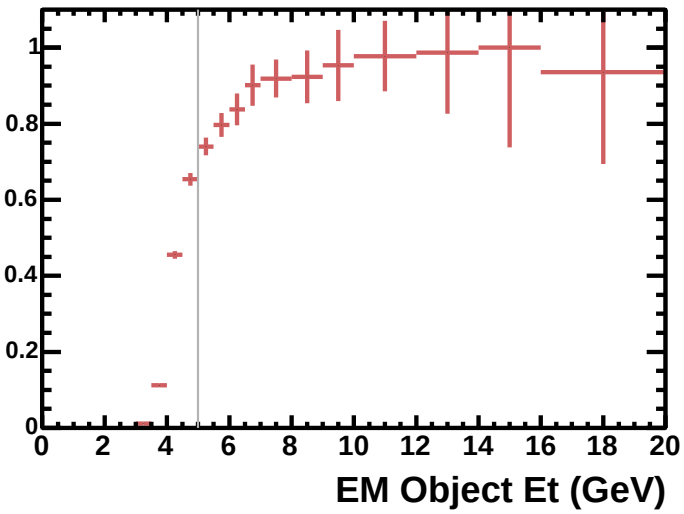

Figure 20: Electron trigger efficiency, $\varepsilon_{e,trig}$, as a function of offline E_T

Electron ID Efficiency

Central Electron ID Efficiency

The simplest way to measure the electron ID efficiency is to obtain a clean (very little background) sample of electrons without using the cuts you wish to examine. The efficiency can then be determined by counting the fraction of electrons from the clean sample that pass the electron ID cuts. To obtain a clean and unbiased sample of electrons, $J/\Psi \rightarrow ee$ events are selected from events that were triggered with only one electron. If the trigger contained two electrons, then there would be a trigger bias in the sample. One of the legs of the J/Ψ is used to tag the J/Ψ , the other is used as a probe to measure the electron efficiency. Efficiency is defined as the number of probe electrons that pass a cut divided by the total number of probe electrons.

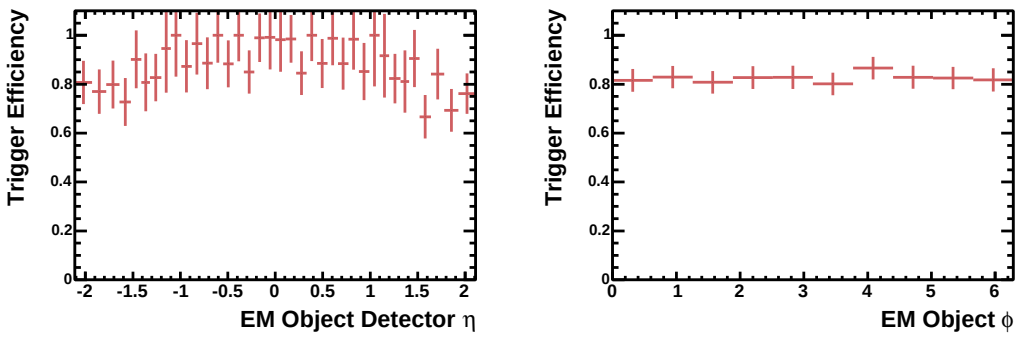

Figure 21: Electron trigger efficiency, $\varepsilon_{e,trig}$, as a function of offline η and ϕ

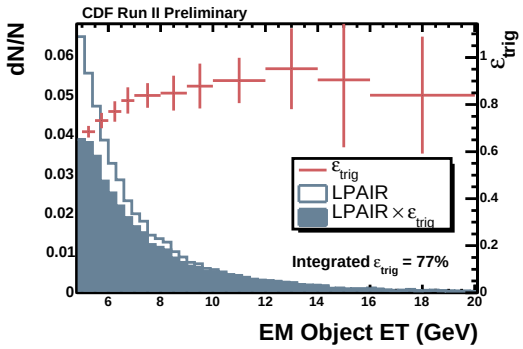

Figure 22: The overall electron trigger efficiency, $\varepsilon_{e,trig}$, is calculated as the integral of the closed histogram divided by the integral of the open histogram.

$$\varepsilon_{e,id} = \frac{N_{e,probe}^{passIDcuts}}{N_{e,probe}} \tag{5}$$

To obtain a clean and unbiased sample of $J/\Psi \rightarrow ee$ events we followed the procedure similar to CDFNOTE 7379 [13]. Using the edil0d dataset stntuplized with CDFSOFT version 5.3.3 and stntuple dev_242, we selected events that passed the ELECTRON_CENTRAL_4 trigger. In order to select J/Ψ events we made the following requirements on the electron objects (TStnElectrons) in the event:

- require 2 or 3 TStnElectrons in the event (to reduce combinatoric background)
- make an array of tight electrons from the TStnElectrons (tight electron cuts are listed in Table 6)
- for each tight electron, match it to a probe electron which has
  - Z vertex within 1 cm of the tight electron

- opposite charge to the tight electron
- in a different tower than the tight electron
- invariant mass between 2.9 GeV/c^2 and 3.3 GeV/c^2

The TStnElectrons that pass all the above requirements are then called "probe electrons". The invariant mass of the tight electrons with the probe electrons (before the mass cut) is shown in Figure 23. This shows a very nice J/Ψ peak with very little background. Therefore the probe electrons fit the requirement of being clean and unbiased because they were selected without trigger or quality cuts and have very little background.

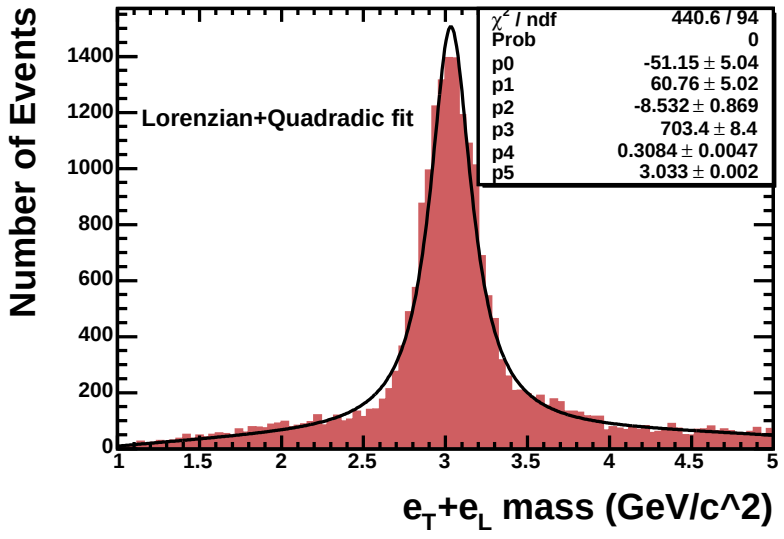

Figure 23: Tight + Loose (ie. probe) electron invariant mass which shows a very clean J/Ψ peak.

The efficiency for the hadem cut is 95%±3%, see Figure 24. The efficiency calculated could be slightly lower than the actual efficiency in an exclusive event because there could be some hadronic activity on top of the electron, increasing the value of hadem for the electron. Efficiency for CES shape cut is 99%±1%, see Figure 25. Combined efficiency for both cuts is 95%±4%, and is independent of E_T , η , and ϕ , as shown in Figure 26

Plug Electron ID Efficiency

The above data set used to calculate the central electron ID efficiency can not simply be extended to look at electrons in the plug, because the trigger is based on a central EM object, and most $J/\Psi \rightarrow ee$ events produce two electrons that are close together - so they are unlikely to have probe electrons in the plug region. Fortunately, a thorough study of plug electrons in the E_T region of interest has already been done [15]. The result is a HadEm efficiency of 99%±1% and a PES shape χ^2 efficiency of 88%±2%, so the total plug electron ID efficiency is 87%±3%.

E_T	> 5.0 GeV
E/p	< 2.0
$\|Z_o\|$	< 60 cm
Had/Em	$< 0.055+0.00045*E$
Iso/Et	< 0.1
Lshr	< 0.2
DelXQ	$>$ -3.0 and < 1.5
DelZ	< 5.0
Chi2Strip	< 10.0
FidEleSmx	$=1$
Nssl and Nasl	> 2

Table 6: Tight electron cuts

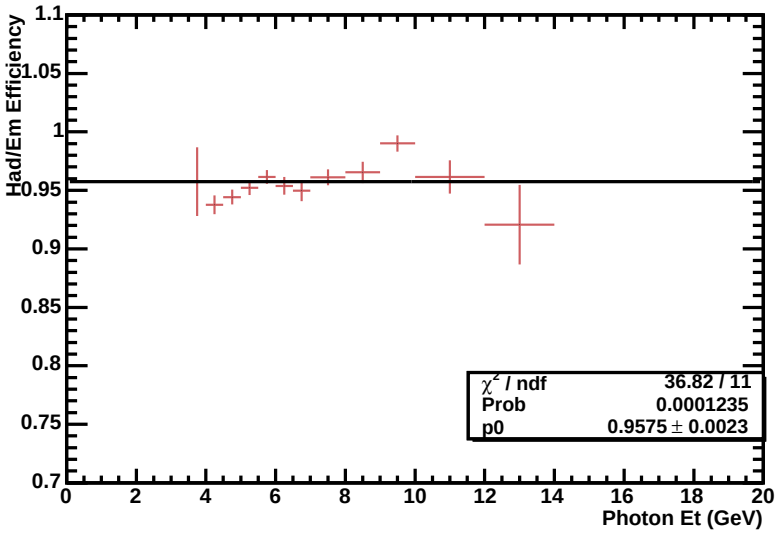

Figure 24: Efficiency of the hadem cut.

Overall Electron ID Efficiency

The overall electron ID efficiency can now be calculated based on the expected fraction of electrons in the central and plug regions. LPAIR MC predicts that 63% of reconstructed electrons with $E_T > 5.0$ GeV and $\eta < 2.0$ fall in the central region, and 37% in the plug region. Weighting the central and plug ID efficiencies by 0.63 and 0.37, the overall electron ID efficiency (per electron) is 0.92±0.04.

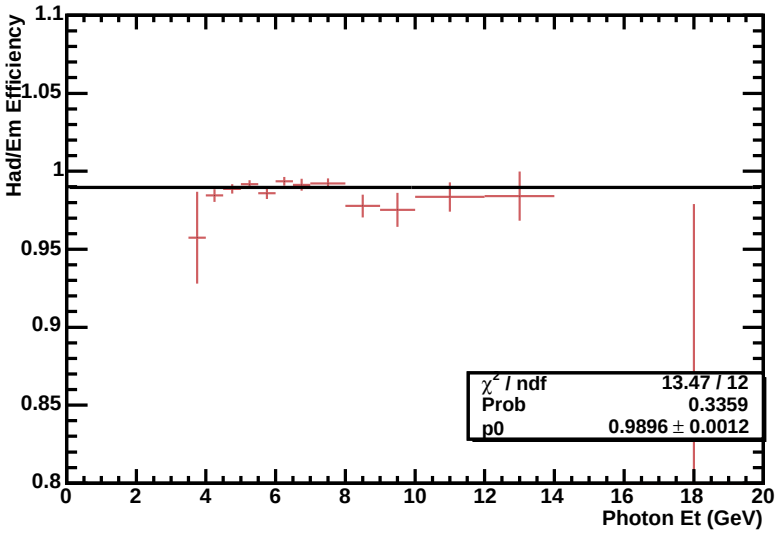

Figure 25: Efficiency of the CES shape cut.

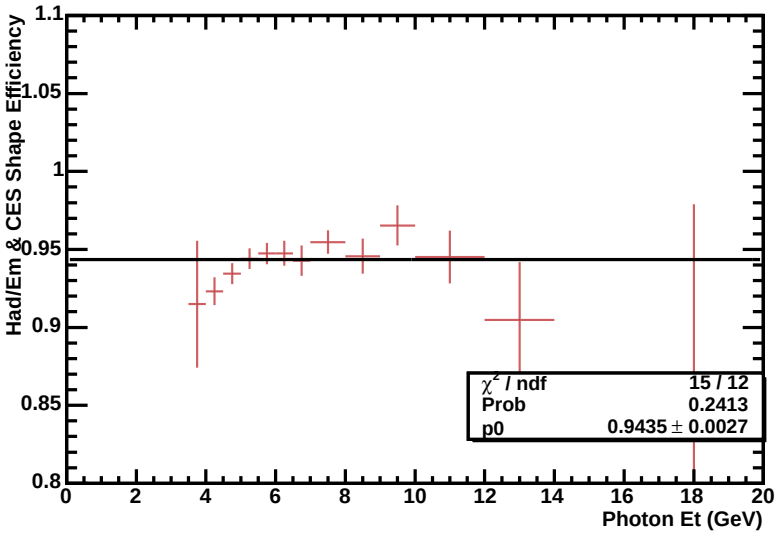

Figure 26: Efficiency of the electron ID cuts (hadem and CES shape).

Electron Tracking Efficiency

The tracking efficiency can be calculated from the same sample of probe electrons used in the ID efficiency. It can be defined as:

$$\varepsilon_{e,id} = \frac{N_{e,probe}^{pass\ track\ cut}}{N_{e,probe}} \tag{6}$$

Where the numerator, $N_{e,probe}^{pass\ track\ cut}$ is the number of probe electrons with NTracks==1 and that track having p_T >1 GeV, and the denominator, $N_{e,probe}$, is the number of probe electrons. The probe electrons in this case are taken from $Z \rightarrow ee$ events where the Z is identified using electrons constructed with their calorimeter properties. If an electron from a pair in the mass window 80 GeV to 100 GeV has a track, then the other electron is used as the probe. Figure 27 shows that the tracking efficiency is ∼99% in the central region, and drops to ∼20% at η =2. This plot is constructed using any tracking algorithms except silicon stand-alone (since silicon is not required in the good run list). The efficiency as a function of η is then integrated with the reconstructed electron η distribution from LPAIR in Figure 28, which shows the overall tracking efficiency is 87% (per electron).

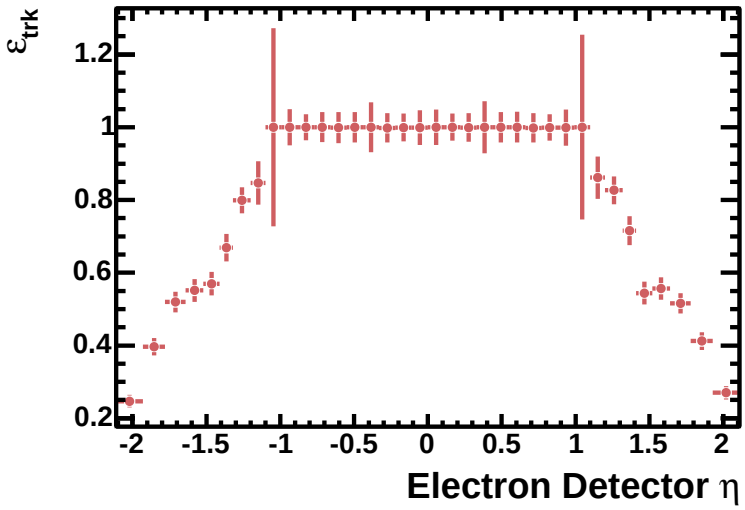

Figure 27: Tracking efficiency.

Overall Electron Efficiency

From the summary of the electron efficiencies shown in Table 7, the overall electron pair efficiency is calculated to be:

$$\varepsilon_{ee} = \varepsilon_{ee,rec} \cdot \varepsilon_{e,trig}^2 \cdot \ \varepsilon_{e,id}^2 \cdot \varepsilon_{e,trk}^2 = 0.26 \pm 0.03 \tag{7}$$

4.2 Final State Radiation Efficiency, ε_{fsr}

If one of the final state electrons in a $p\bar{p} \rightarrow p + ee + \bar{p}$ interaction emits enough bremsstrahlung radiation, it is possible for there to be energy deposited outside the electron towers. This would prevent the event from being counted as signal event because all energy outside the electron towers is vetoed in the exclusive cuts. This is not accounted for in ε_{exc} because that is based entirely on the state of the detector,

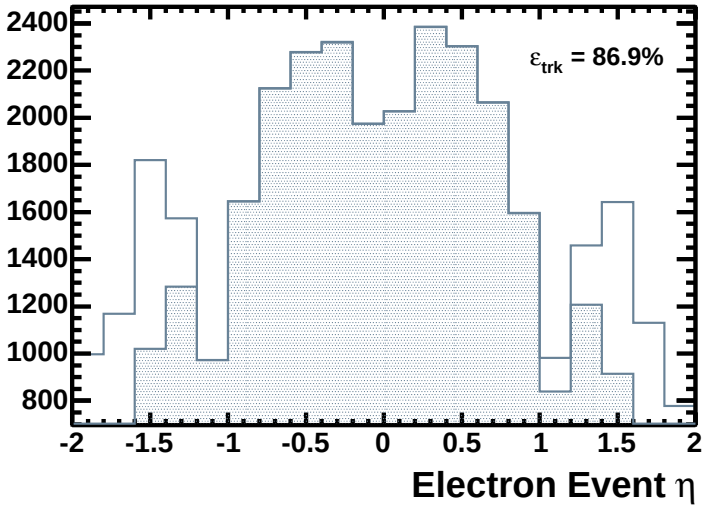

Figure 28: LPAIR η distribution (empty histogram) and the LPAIR η distribution weighted by the tracking efficiency in that η bin (filled histogram).

$\varepsilon_{ee,rec}$	0.69±0.02
$\varepsilon_{e,trig}$	0.77±0.05
$\varepsilon_{e,id}$	0.92 ± 0.04
$\varepsilon_{e,track}$	0.87 ± 0.05
ε_{ee}	0.26 ± 0.03

Table 7: Summary of electron efficiencies

not the details of the signal. To estimate ε_{fsr} we run a sample of LPAIR Monte Carlo events through the exclusive cuts. ε_{fsr} can then be defined as:

$$\varepsilon_{fsr} = \frac{N_{MC\ events}^{pass\ exc\ cuts}}{N_{MC\ events}} \tag{8}$$

Where the denominator, $N_{MC\ events}$ is the number of LPAIR events with both electrons in $|\eta| < 2$. The numerator is the number of denominator events that pass the exclusive cuts described in the event selection, Section 3.4, giving ε_{fsr}=0.79±0.05.

4.3 Cosmic Efficiency, ε_{cos}

The efficiency of the cosmic cut is determined by selecting a sample of non-cosmic electron pairs with the following cuts:

- track $D_0 < 2$ cm

- track pair $\Delta Z_0 < 1.0$ cm
- 3-D opening angle < 2.6 rad
- Seed Tower $<$ tower 18 (EM Timing is not available for towers 18 and greater)

The cosmic efficiency, ε_{cos}, is then defined as:

$$\varepsilon_{cos} \equiv \frac{\#\ non-cosmic\ events\ pass\ cosmic\ cut}{\#\ non-cosmic\ events} \tag{9}$$

A plot of the EM time for non-cosmic events is shown in Figure 29. 93% of anticosmic events have both electrons within cut window, therefore, $\varepsilon_{cos} = 0.93 \pm 0.03$. A systematic was evaluated by shifting the cosmic cut by the resolution of the EM timing system. The events in the -99 bin are events that did not have EM timing information available - this is the source of the inefficiency. The dominant reason for electrons to not have EM timing information is that the tower energy is below the threshold for EM timing information (4GeV).

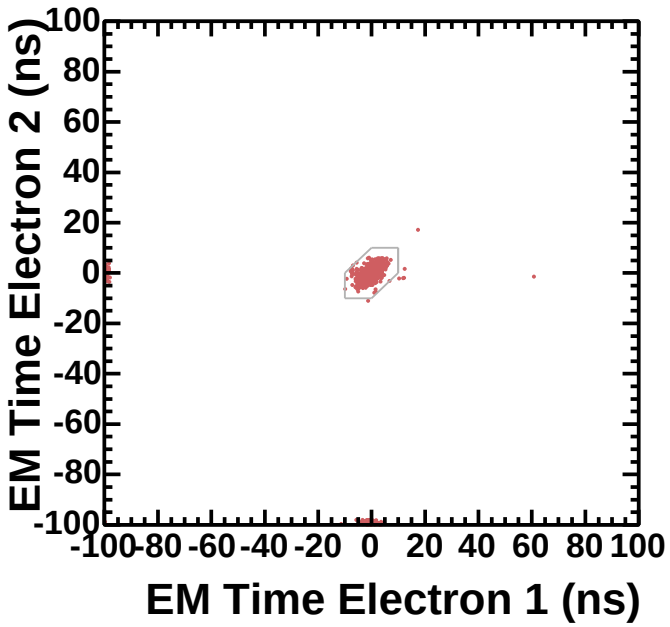

Figure 29: EM time of electron 1 vs. electron 2 for non-cosmic events are plotted. Bin -99 corresponds to events with no EM timing information available. ε_{cos}=0.93±0.03

4.4 Exclusive Efficiency

In a cross section calculation, efficiencies are normally multiplied by the integrated luminosity, for example $\varepsilon_x \cdot \int \mathscr{L}_{inst} dt$. However, since ε_{exc} depends on the instantaneous

luminosity it must be put into the luminosity integration $\int \varepsilon_{exc} \cdot \mathscr{L}_{inst} dt$. At CDF, $\mathscr{L}_{inst}$is normally defined as the sum of the instantaneous luminosities of the 36 bunches circulating in the Tevatron. This definition is not quite adequate for this analysis, because it is the instantaneous luminosity of the bunch that determines the exclusive efficiency. To deal with this bunch by bunch luminosity correction, a weight, W_b, for each bunch in a run is extracted from the database. This weight is the luminosity of the bunch relative to the mean luminosity of the 36 bunches ($W_b = \frac{\mathscr{L}_{bunch}}{\langle \mathscr{L}_{bunch} \rangle}$). Using this presciption requires the assumption that the W_b remains constant for the duration of the run. By looking at W_b at the begining and end of a very long run, the assumption that it remains constant can be tested. The bunch weight stays constant to within 5% in run 206537[7]. This means that the presciption is valid and the effective luminosity, $\mathscr{L}_{eff}$, is therefore defined as:

$$\mathscr{L}_{eff} = \int \varepsilon_{exc} \cdot \mathscr{L}_{bunch} dt \tag{10}$$

Where $\mathscr{L}_{bunch} = W_b \cdot \mathscr{L}_{inst}/36$, and ε_{exc} is the exclusive efficiency, defined as:

$$\varepsilon_{exc} \equiv \frac{N_{exc}^{observed}}{N_{exc}^{truth}} = 1 - \frac{N_{exc}^{spoiled}}{N_{exc}^{truth}} \tag{11}$$

where $N_{exc}^{observed}$ is the number of exclusive interactions observed in the data sample, N_{exc}^{truth} is the true number of exclusive interactions in the data sample, and $N_{exc}^{spoiled} = N_{exc}^{truth} - N_{exc}^{observed}$. An exclusive interaction can be spoiled by another inelastic $p\bar{p}$ interaction in the beam crossing, a particle entering the detector that was not part of an interaction (beam halo or cosmic), or noise in any of the detectors used to define the exclusive interaction (the calorimeters and BSC).

In order to calculate the fraction $\frac{N_{exc}^{spoiled}}{N_{exc}^{truth}}$ one must assume that the probability of an exclusive interaction occuring in a beam crossing is independent of any of the factors that can spoil it (cosmic ray, beam halo, noise, or multiple inelastic interaction occuring in the same beam crossing). With that assumption and the definition that the final state of an exclusive interaction contains only the outgoing hadrons and the central system (ie. two electrons), the following is deduced:

$$\frac{N_{exc}^{spoiled}}{N_{exc}^{truth}} = \frac{N_{BC}^{spoiled}}{N_{BC}} \tag{12}$$

where $N_{BC}^{spoiled}$ is the number of beam crossings with any effect that would spoil the ability to observe the exclusivity of an interaction, and N_{BC} is the total number of beam crossings. In other words, the exclusive efficiency is the probability that an exclusive interaction could be observed in the detector if an exclusive interaction occured. From equations 11 and 12, and the fact that zerobias data is an unbiased sample of beam crossings:

$$\varepsilon_{exc} = 1 - \frac{N_{BC}^{spoiled}}{N_{BC}^{total}} = 1 - \frac{N_{ZB}^{fail}}{N_{ZB}^{total}} = \frac{N_{ZB}^{pass}}{N_{ZB}^{total}} \tag{13}$$

where $N_{ZB}^{fail(pass)}$ is the number of zerobias events that fail (pass) all of the exclusive cuts, and N_{ZB}^{total} is the total number of zerobias events in the data sample. Of course,

[7]initial luminosity = 125×10^{30} cm^{-2}s^{-1}, final luminosity = 18×10^{30} cm^{-2}s^{-1}, duration = 25 hours

$N_{ZB}^{pass} = N_{ZB}^{total} - N_{ZB}^{fail}$, therefore

$$\varepsilon_{exc} = \frac{N_{ZB}^{pass}}{N_{ZB}^{total}} \tag{14}$$

This is how ε_{exc} is determined from data. It is important to do this over the same run range as the data, since the beam effects and electronic noise are run dependent. Figure 30 is a plot of ε_{exc} as a function of bunch luminosity for the same good run list used for the event selection. Figure 31 shows the n-1 exclusive efficiency for each detector region.

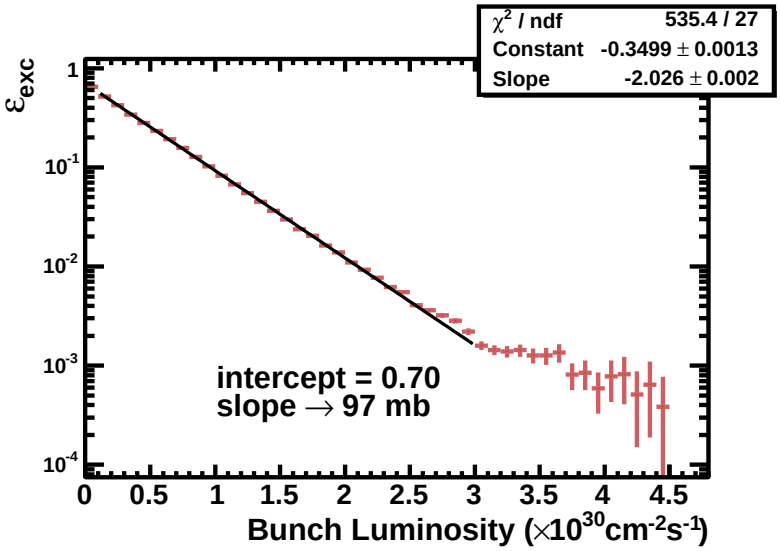

Figure 30: Exclusive efficiency as a function of bunch luminosity. The fit curve is only a guide, it is not used to calculate the effective luminosity. The slope and intercept calculation shown indicate the level of inefficiency; if the cuts were perfect the intercept would be 1.0 and the cross section would be 60mb. The higher σ indicates that the cuts are conservative.

Now that ε_{exc} is calculated, we can calculate $\mathscr{L}_{eff}$with Figure 32. The open histogram is the $\mathscr{L}_{bunch}$distribution for all zerobias data in the good run range weighted by the bunch luminosity, the points are ε_{exc} (note that the scale for ε_{exc} is on the right), and the filled histogram is the weighted $\mathscr{L}_{bunch} \times \varepsilon_{exc}$. The effective luminosity is equal to the integral of the filled histogram ($\int \varepsilon_{exc} \cdot N \; d\mathscr{L}$), divided by the integral of the open histogram ($\int \cdot N \; d\mathscr{L}$), multiplied by the total integrated luminosity of the good run list ($\int \mathscr{L} \; dt$). This is mathematically demonstrated in Appendix 7.4.

$$\mathscr{L}_{eff} = \frac{\int \varepsilon_{exc} \cdot N \; \cdot \mathscr{L} d\mathscr{L}}{\int N \cdot \mathscr{L} \; d\mathscr{L}} \int \mathscr{L} \; dt \tag{15}$$

$$\mathscr{L}_{eff} = 0.0856 \cdot 532 \pm 32 pb^{-1} = 46 \pm 3 pb^{-1} \tag{16}$$

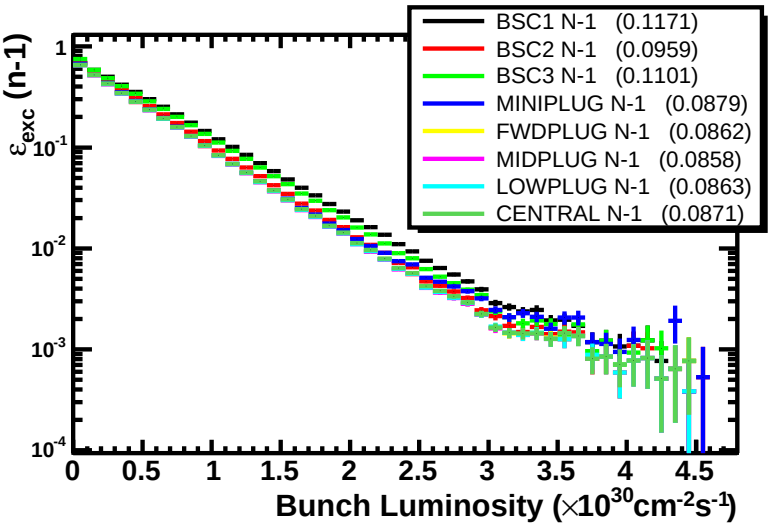

Figure 31: The n-1 efficiency as a function of instantaneous luminosity for each of the exclusive cuts.

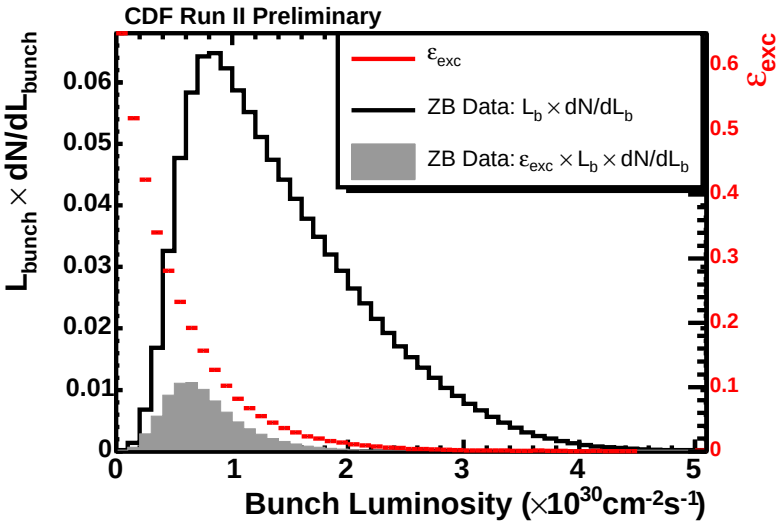

Figure 32: $\mathscr{L}_{bunch}$distribution for all zerobias data (open histogram with scale on left), ε_{exc} (points with scale on right), and weighted $\mathscr{L}_{bunch} \times \varepsilon_{exc}$ (filled histogram with scale on left) for calculation of $\mathscr{L}_{eff}$

5 Backgrounds

There are four backgrounds to consider.

'jet' fake background due to something other than an electron appearing to be an

electron by passing the electron cuts

cosmic background due to cosmic rays occuring in time with the beam crossing

exclusivity background due to inclusive processes (ie. Drell-Yan) that are observed as exclusive due to particles not being observed in the calorimeters (ie. falling into cracks in the detector or being too soft to reach any detectors)

dissociation background due to inelastic e^+e^- events where the dissociation products are too far forward to be detected by the BSCs.

5.1 'Jet' Fake Background

The jet fake rate (F_{jet}) is the probability that a hadron fakes an electron by passing the electron cuts. The jet fake rate for this analysis is defined as the probability that a single-track jet[8] passes the electron cuts.

$$F_{jet} \equiv \frac{N_{jets}^{pass\ electron\ cuts}(|\eta| < 2,\ NTracks = 1,\ TrackPt > 1.0)}{N_{jets}(|\eta| < 2,\ NTracks = 1,\ TrackPt > 1.0)} \tag{17}$$

Where the denominator, $N_{jets}(|\eta| < 2,\ NTracks = 1,\ TrackPt > 1.0)$ is the number of jets in GAP_GAP_ST5 trigger data (the same good run list as the signal sample) with $|\eta| < 2,\ NTracks = 1,\ TrackPt > 1.0$. The numerator, $N_{jets}^{pass\ electron\ cuts}(|\eta| < 2,\ NTracks = 1,\ TrackPt > 1.0)$ is the number of denominator jets that pass the electron cuts listed in Table 2 plus the single-track with p_T >1.0 GeV requirement. Figure 33 shows F_{jet} is <2%[9], and does not have significant dependence on E_T .

Naively, the jet fake background could be estimated by estimating the number of events with two exclusive jets expected in the data sample, $N_{jj}^{pass\ all\ exc\ cuts}$, and then weighting each jet by F_{jet}. However, F_{jet} is a calculation of the ratio of *inclusive* jets faking electrons, not *exclusive* jets faking electrons. This means that we can not apply the exclusivity requirement to the jet if we want to weight it by F_{jet}. To avoid this difficulty, F_{jet} will be applied to all jets in the GAP_GAP_ST5 trigger data that pass the exclusivity cuts in the $|\eta| > 2$ region. This means that we will get an upper limit on the jet fake background, since $N_{jj}^{pass\ all\ exc\ cuts} < N_{jj}^{pass\ |\eta|>2\ exc\ cuts}$, while avioding the application of the exclusivity requirement to the jets which are all in $|\eta| < 2$.

There are 0 events in the GAP_GAP_ST5 trigger data with two single-track jets passing the exclusive cuts for $|\eta| > 2$. Therefore, to 95% CL, there are less than 3.1 events with two single-track jets and pass the exclusive cuts. However, there is a factor 100 prescale on the GAP_GAP_ST5 trigger, therefore $N_{jj}^{pass\ all\ exc\ cuts} < 310$. Applying F_{jet} to each jet, gives an upper limit of $310 \cdot (0.02)^2 = 0.12$ background events. This estimate is an upper limit, so the jet fake background is $0.0^{+0.1}_{-0.0}$ events.

[8] 'single-track' is specified because a multi-track jet does not fake the signal which requires only 1 track

[9] the numerator 'jets' could actually be electrons

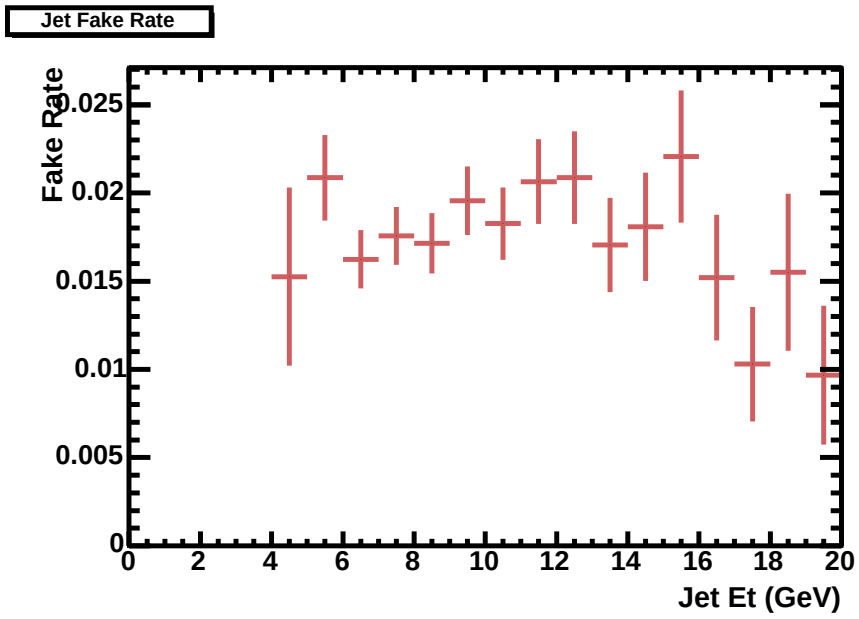

Figure 33: Jet fake rate (F_{jet}) is <2%

5.2 Cosmic Background

The background from cosmic rays falling within the cosmic cuts can be evaluated by measuring the density of events outside the cosmic cuts and then extrapolating that density into the cut region. Figure 34 is a plot of the EM time of all electron candidates (with no track cut) in the DIFF_DIPHOTON trigger sample (black) and the non-cosmic events (red). There are 514 events in the 9700 ns^2 area outside the signal region, so the density of background events is 0.0530 events/ns^2. The signal region is 300 ns^2, so we can expect 15.9 of the 67502 events in signal region to be cosmic. Therefore the probability of a two electron event that passes the cosmic cuts acutally being a cosmic is 2.3×10^{-4}. This corresponds to a negligible number of background events in the 16 event signal sample.

5.3 Exclusivity Background

The exclusivity background accounts for non-exclusive events where some particle(s) passed through the cracks in the calorimetry coverage or below the noise thresholds, causing them to appear exclusive. Z boson events provide an ideal sample to test the ability of the calorimeters to observe exclusive events because Z can not be produced exclusively[10], and it decays to two electrons. Events from the two candidate sample (with tracks) are compared to Z events as a function of the number of associated towers[11] in Figure 35.

Figure 35 shows a very clear peak above a very small background. In order to estimate the amount of background in the zero bin (the signal region), the number of

[10] it can not be produced exclusively via two-photon nor gluon exchange.

[11] An associated tower is a tower that is not an electron tower but is above the exclusive cut threshold.

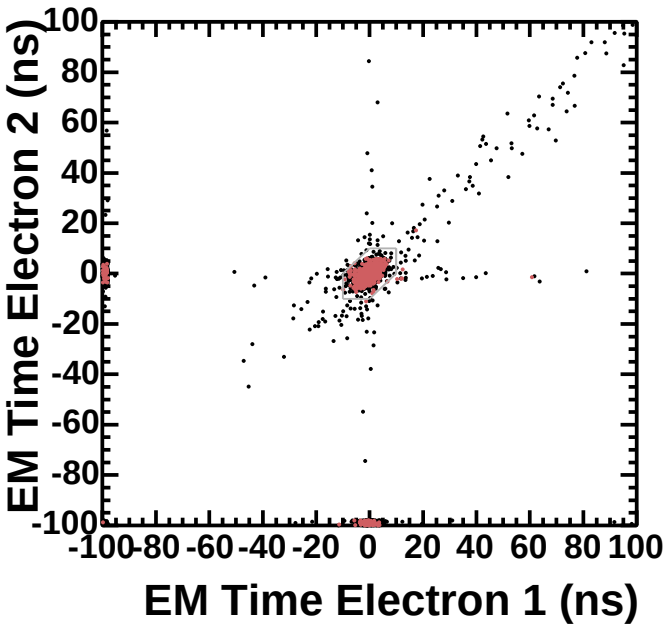

Figure 34: The cosmic background fraction is estimated to be 2.3×10^{-4}.

events in the 5 to 20 bins are averaged over all 15 bins. 3 events in 15 bins, comes out to 0.2 events per bin. Because there is no real evidence the exclusive background acutally results in any background events, this estimate is taken as an upper limit, making the exclusivity background $0.0^{+0.2}_{-0.0}$.

A potentially significant difference between the signal sample of this analysis and the Z→ee data is the E_T of the electrons being considered. Z→ee electrons have much higher E_T than those in the signal sample. To investigate this potential complication, a Drell-Yan MC was used in place of the Z→ee data in Figure 36. It shows the same result, a very small background on top a very clear peak. This is a cross check, not an additional background, so it does not add anything but confidence to the previous background estimate.

5.4 Dissociation Background

The dissociation background accounts for events that are mediated by two-photon exchange, but instead of being truly exclusive, one or both of the protons is excited into a low mass state and then dissociates. It is possible for these dissociations to be contained inside the beam pipe, and hence they would not be observable in the CDF detector. The inelastic running mode of LPAIR MC is used to estimate this background. Unfortunately, LPAIR MC only provides the kinematics of the dissociating proton, it does not actually dissociate the system. To dissociate the system, a function called 'fragment_cluster' from Minimum Bias Rockefeller (MBR) MC is used. This function fragments a cluster into pions, and then boosts the system back into the lab frame. Figure 37 shows the η distribution of cluster fragments and the fraction of proton dissociations whose fragments would all remain in the region greater than the η cut. The right hand plot shows that 7% of dissociating protons from LPAIR events

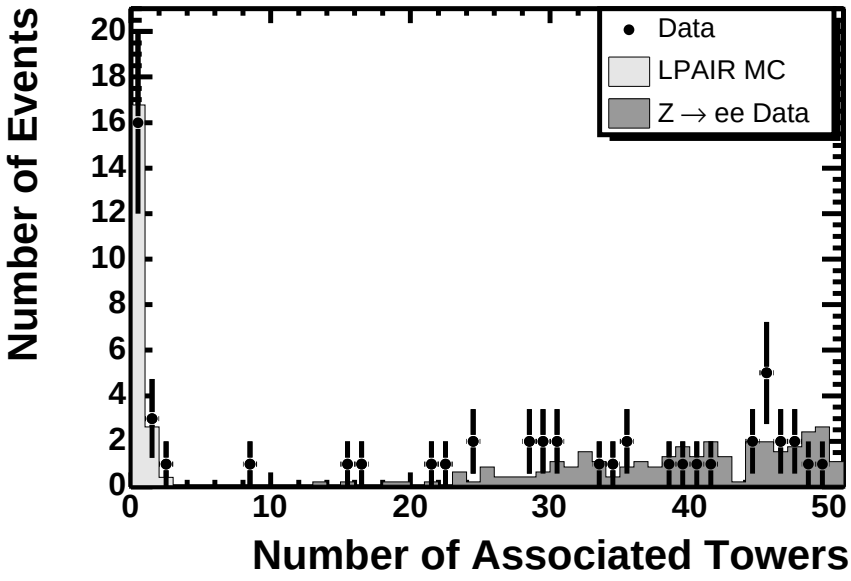

Figure 35: Number of associated towers for LPAIR MC, Z→ee data, and the electron sample (with no BSC cuts applied). LPAIR MC is normalized to events below 5 towers, Z→ee data is normalized to the events above 5 towers.

with electrons in $E_T > 5.0$ GeV and $\eta < 2.0$ have no particles with $\eta < 7.4$.

To get the probability of a blind dissociation[12], P_{BD}, the efficiency of the BSC 3 counters, ε_{BSC3} must be taken into account. In order to determine ε_{BSC3} minbias data was examined for events that had a hit in one of the PMTs in the counter when a hit was present in the other PMT in that same counter. Figure 38 shows the efficiency for each of the 4 PMTs in BSC3 (2 PMTs on east side, 2 PMTs on west side) is 0.9±0.1. Since the denominator is does not always correspond to a particle in the channel, this efficiency is really an upper limit. Therefore, $P_{BD} = 0.07/0.9 = 0.08 \pm 0.01$.

To determine how many background events this corresponds to, P_{BD} must be factored into the cross section for the proton dissociation events. LPAIR MC predicts that $\sigma_{inel-el} = 1.54pb$, $\sigma_{inel-inel} = 1.48pb$, and $\sigma_{el-el} = 1.71pb$. Taking these and P_{BD} into account, the cross section for a blind dissociation event is $\sigma_{BD} = 0.25$pb[13]. All events in the candidate sample correspond to $\sigma_{Cand} = 1.71 + 0.25 = 1.96pb$, so the fraction of events in the candidate sample is F_{BD}=0.13±0.02, where the uncertainty comes from the systematic on P_{BD}, since the uncertainties on the LPAIR predicted cross sections are negligible. This corresponds to 2.1±0.3 events in the 16 events of the signal sample.

5.5 Background Summary

A summary of the backgrounds is listed in Table 8.

[12]blind dissociation meaning a dissociation that was not observed in the BSC

[13]$\sigma_{BD} = 2P_{BD}\sigma_{inel-el} + P_{BD}^2\sigma_{inel-inel} = 0.25pb$

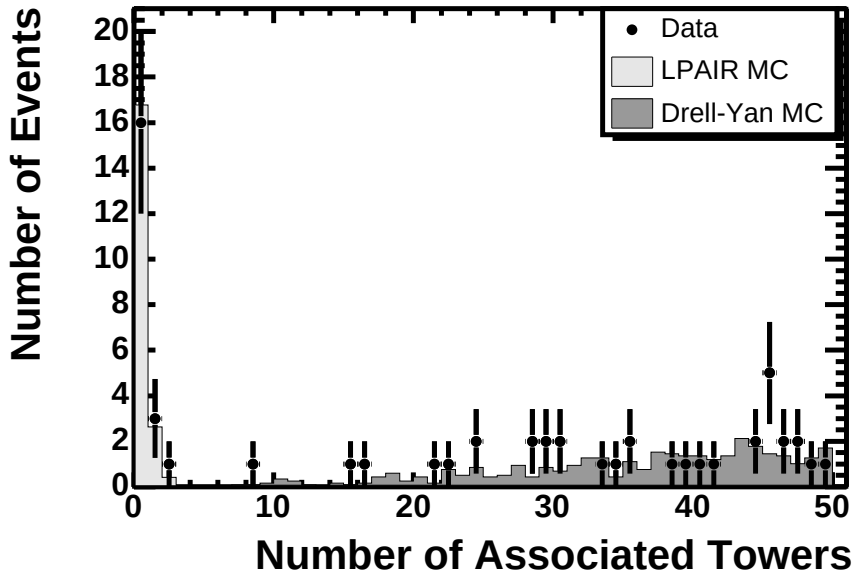

Figure 36: Number of associated towers for LPAIR MC, Drell-Yan MC, and the electron sample. LPAIR MC is normalized to events below 5 towers, Drell-Yan MC is normalized to the events above 5 towers.

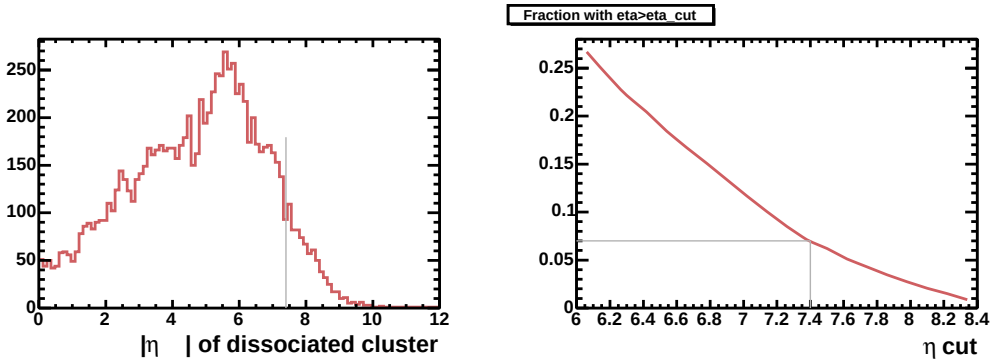

Figure 37: η distribution of cluster fragments (left), fraction of proton dissociations whose fragments would all remain in region greater than the η cut.

6 Cross Section

Using Equation 18 and the numbers in Table 9 the cross section for exclusive ee (E_T >5 GeV, $\eta < 2$) is measured to be $\sigma_{exc,ee}^{E_t>5\ GeV,\eta<2} = 1.6^{+0.5}_{-0.3}(stat) \pm 0.3(sys)pb$. **This agrees with the theoretical cross section from LPAIR of 1.711±0.008 pb.**

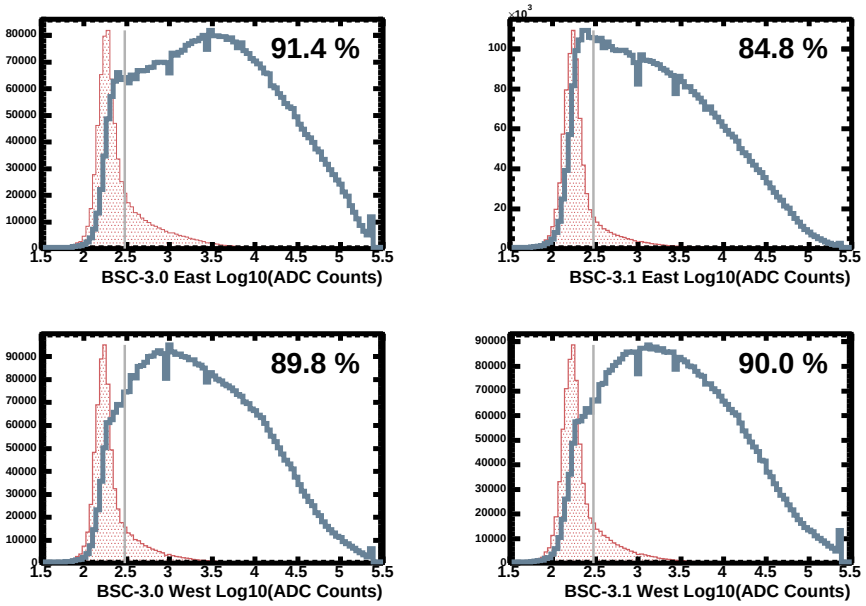

Figure 38: Plots show the number of events with a hit (ADC counts>400) in a PMT, given that there was (empty histogram) or was not (filled histogram) a hit in the adjacent PMT. The efficiency is the fraction of events in the empty histogram above 400 counts divided by the number of events in the empty histogram.

Background	Value	Systematic
jet fake	0.0	$^{+0.1}_{-0.0}$
cosmic	negligible	negligible
exclusive	0.0	$^{+0.2}_{-0.0}$
dissociation	2.1	0.3
total	2.1	$^{+0.6}_{-0.3}$

Table 8: Summary of background numbers put into the cross section calculation.

$$\sigma_{exc,ee}^{E_t>5\ GeV,\eta<2} = \frac{N_{sig} - N_{bkgd}}{\varepsilon_{cos} \cdot \varepsilon_{fsr} \cdot \varepsilon_{ee} \cdot \varepsilon_{exc} \cdot \mathscr{L}} \tag{18}$$

Summary and Conclusions

We have observed 16 exclusive electron pair events in CDF, within $|\eta_e| < 2.0$ and $p_T > 5$ GeV/c with a background estimate of 2.1 $^{+0.6}_{-0.3}$ events. The events are consistent in both their cross section and kinematic distributions with

Quantity	Value	Uncertainty
N_{sig}	16	$^{+5.1}_{-3.2}$ (stat)
N_{bkgd}	2.1	$^{+0.6}_{-0.3}$ (sys)
$\mathscr{L}$	532	32 (sys)
ε_{exc}	0.0856	n/a
ε_{cos}	0.93	0.03 (sys)
ε_{fsr}	0.79	0.05 (sys)
ε_{ee}	0.26	0.03 (sys)

Table 9: Summary of numbers put into the cross section calculation.

$pp \to p + e^+e^- + p$ through two photon exchange ($\gamma\gamma \to e^+e^-$). There is a 3.0×10^{-8} probability that the this is a background fluctuation, corresponding to a 5.5σ observation. This is the first time the two-photon process has been observed in hadron-hadron collisions.

Acknowledgements

We would like to acknowledge the significant effort by the Rockefeller group to install and maintain the forward detectors that are essential for this analysis. We would also like to thank the hard work of the QCD conveners and the analysis reviewers for carefully examining this analysis.

7 Appendicies

7.1 Appendix: L3 Trigger χ^2 Correction

There was a bug in the Level 3 Trigger (L3) summary bank χ^2 variable, `TL3Em::CesAvgChi2()`. The value cut on in L3 was not the same value that was recorded in the L3 summary bank. To solve this problem, I reconstructed the L3 value of the χ^2 in the following way. The corrected χ^2 is calculated using Equation 19

$$\chi^2 = S(E) \cdot \chi^2_{uncorr} \qquad \textbf{where } S(E) = 0.1792 \cdot 2.11^{log(E)} \tag{19}$$

The offline value of the χ^2 can be slightly different from the L3 value because L3 and offline energies can be different. Knowing the offline χ^2, the offline energy, and the L3 energy[14], the L3 χ^2 can be determined using Equation 20

$$\chi^2_{L3} = \frac{S(E_{L3})}{S(E_{offline})} \cdot \chi^2_{offline} \tag{20}$$

[14]The energy of the L3 object needed to reconstructed from the object's E_T using the CESZ() variable and radius of the CES=184.15cm

7.2 Appendix: Angela's Spike Killer

cf. Angela's J/Psi note cdf6646

The cental calorimeter is known to have PMT spikes in it. Fortunately, these can be vetoed because two PMTs are used to detect the light produced in each tower. Requireing energy in both of these effectively rejects spikes. Spikes in towers with E > 500 MeV are already killed in CalData using this method. The extension of this to lower energyies was studied by taking a sample of events from a cosmic run without beam which were triggered by the zero-bias trigger and no tothers. The distribution of the tower energies is shown in Figure 39. None of the towers have both PMT towers fired.

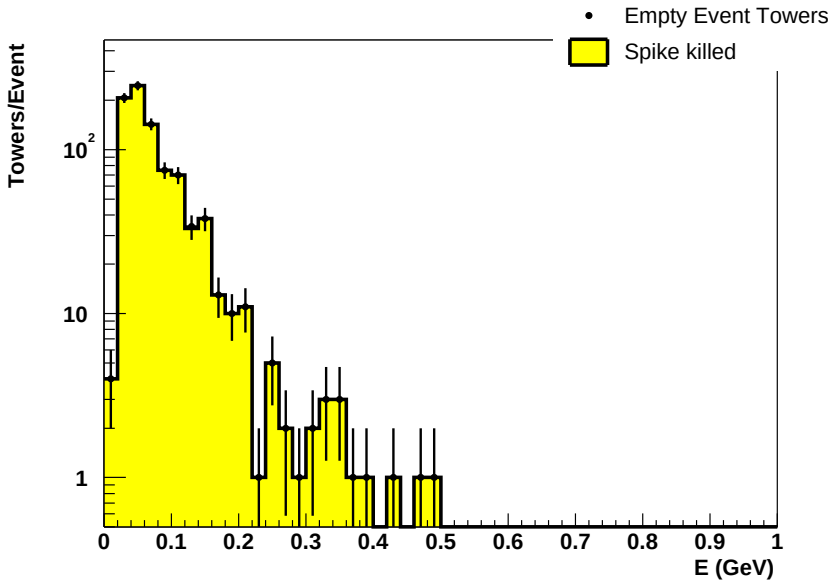

Figure 39: Angela's spike killer

7.3 Appendix: Signal Events Summary

```
Run: 191089 Event: 127812
 Electron 1: (Q)Pt=(1e+06)1e+06 Et=6.825 det eta=0.4429 eta=0.4429 phi=6.111
 Electron 2: (Q)Pt=(1e+06)1e+06 Et=5.864 det eta=0.1948 eta=0.1948 phi=2.827
 dphi=2.999 angle=2.487 mass=12.7 xiP=0.009058 xiPbar=0.004698
Run: 191425 Event: 284590
 Electron 1: (Q)Pt=(-1)8.373 Et=8.701 det eta=-0.1953 eta=-0.3083 phi=6.118
 Electron 2: (Q)Pt=(1)8.849 Et=8.547 det eta=-0.4443 eta=-0.5483 phi=2.985
 dphi=3.133 angle=2.281 mass=17.37 xiP=0.005781 xiPbar=0.01359
Run: 191596 Event: 1594224
 Electron 1: (Q)Pt=(-1)16.9 Et=16.52 det eta=-0.4397 eta=-0.2002 phi=1.528
 Electron 2: (Q)Pt=(1)10.76 Et=8.954 det eta=-0.5466 eta=-0.3176 phi=4.675
 dphi=3.137 angle=2.674 mass=24.36 xiP=0.01023 xiPbar=0.01657
Run: 195762 Event: 3788
 Electron 1: (Q)Pt=(-1)12.07 Et=15.23 det eta=0.3189 eta=0.3901 phi=5.879
 Electron 2: (Q)Pt=(1)10.26 Et=14.59 det eta=0.06644 eta=0.1418 phi=2.708
```

```
 dphi=3.112 angle=2.632 mass=29.98 xiP=0.02006 xiPbar=0.01172
Run: 196752 Event: 1657477
 Electron 1: (Q)Pt=(-1)5.622 Et=6.305 det eta=0.7683 eta=0.8119 phi=2.232
 Electron 2: (Q)Pt=(1)6.252 Et=6.188 det eta=0.6686 eta=0.7148 phi=5.414
 dphi=3.102 angle=1.764 mass=12.5 xiP=0.0137 xiPbar=0.002973
Run: 197657 Event: 13796201
 Electron 1: (Q)Pt=(1)1.797 Et=8.385 det eta=-0.4718 eta=-0.4718 phi=5.451
 Electron 2: (Q)Pt=(-1)8.22 Et=7.798 det eta=-1.222 eta=-1.222 phi=2.304
 dphi=3.135 angle=2.006 mass=17.19 xiP=0.003841 xiPbar=0.02037
Run: 197763 Event: 7914309
 Electron 1: (Q)Pt=(-1)7.706 Et=7.479 det eta=-0.4525 eta=-0.3491 phi=3.3
 Electron 2: (Q)Pt=(1)7.617 Et=7.338 det eta=0.5522 eta=0.6463 phi=0.1483
 dphi=3.131 angle=2.954 mass=16.71 xiP=0.009837 xiPbar=0.007371
Run: 198514 Event: 14359480
 Electron 1: (Q)Pt=(-1)5.636 Et=6.101 det eta=0.06527 eta=0.1506 phi=4.85
 Electron 2: (Q)Pt=(1)6.345 Et=5.471 det eta=0.8558 eta=0.9164 phi=1.669
 dphi=3.102 angle=2.18 mass=12.31 xiP=0.0106 xiPbar=0.003794
Run: 200284 Event: 346775
 Electron 1: (Q)Pt=(1)3.003 Et=5.414 det eta=0.6686 eta=0.6686 phi=1.66
 Electron 2: (Q)Pt=(1e+06)1e+06 Et=5.002 det eta=-0.06527 eta=-0.06527 phi=4.858
 dphi=3.085 angle=2.604 mass=11.2 xiP=0.007781 xiPbar=0.004139
Run: 200570 Event: 4578964
 Electron 1: (Q)Pt=(1)5.67 Et=5.706 det eta=-0.749 eta=-0.7167 phi=5.087
 Electron 2: (Q)Pt=(-1)4.6 Et=5.123 det eta=-1.494 eta=-1.456 phi=1.93
 dphi=3.125 angle=1.372 mass=11.67 xiP=0.002031 xiPbar=0.01717
Run: 201155 Event: 151042
 Electron 1: (Q)Pt=(-1)19.2 Et=19.3 det eta=0.4639 eta=0.3315 phi=4.838
 Electron 2: (Q)Pt=(1)17.51 Et=18.83 det eta=0.2576 eta=0.117 phi=1.69
 dphi=3.135 angle=2.656 mass=38.41 xiP=0.02451 xiPbar=0.01561
Run: 194810 Event: 2697466
 Electron 1: (Q)Pt=(1)7.163 Et=7.829 det eta=-0.7749 eta=-0.794 phi=2.248
 Electron 2: (Q)Pt=(1e+06)1e+06 Et=6.104 det eta=-1.47 eta=-1.493 phi=5.435
 dphi=3.096 angle=1.274 mass=14.65 xiP=0.002506 xiPbar=0.02269
Run: 199189 Event: 6276945
 Electron 1: (Q)Pt=(1e+06)1e+06 Et=5.999 det eta=-0.4429 eta=-0.4429 phi=1.912
 Electron 2: (Q)Pt=(1e+06)1e+06 Et=5.123 det eta=0.2188 eta=0.2188 phi=5.054
 dphi=3.141 angle=2.962 mass=11.76 xiP=0.005218 xiPbar=0.006866
Run: 200056 Event: 10189203
 Electron 1: (Q)Pt=(-1)7.127 Et=7.284 det eta=0.8668 eta=0.7948 phi=5.672
 Electron 2: (Q)Pt=(1)27.52 Et=6.664 det eta=1.718 eta=1.622 phi=2.521
 dphi=3.133 angle=1.226 mass=15.31 xiP=0.02544 xiPbar=0.00235
Run: 200056 Event: 12978584
 Electron 1: (Q)Pt=(1e+06)1e+06 Et=5.603 det eta=-0.6753 eta=-0.6753 phi=5.873
 Electron 2: (Q)Pt=(1e+06)1e+06 Et=5.327 det eta=-0.6802 eta=-0.6802 phi=2.792
 dphi=3.08 angle=1.863 mass=10.92 xiP=0.002832 xiPbar=0.01098
Run: 200309 Event: 4426144
 Electron 1: (Q)Pt=(1e+06)1e+06 Et=9.849 det eta=2.031 eta=2.089 phi=0.2948
 Electron 2: (Q)Pt=(-1)9.84 Et=9.075 det eta=1.254 eta=1.306 phi=3.42
 dphi=3.126 angle=0.7709 mass=20.66 xiP=0.05769 xiPbar=0.001876
Run: 200719 Event: 7411538
 Electron 1: (Q)Pt=(1)6.65 Et=6.276 det eta=-0.3212 eta=-0.001579 phi=2.994
 Electron 2: (Q)Pt=(-1)7.014 Et=5.836 det eta=1.361 eta=1.614 phi=6.103
 dphi=3.109 angle=1.976 mass=16.17 xiP=0.01815 xiPbar=0.0038
```

```
Run: 201371 Event: 1580716
 Electron 1: (Q)Pt=(1)5.229 Et=5.288 det eta=0.7675 eta=0.8153 phi=2.082
 Electron 2: (Q)Pt=(1e+06)1e+06 Et=5.048 det eta=1.237 eta=1.288 phi=5.21
 dphi=3.128 angle=1.414 mass=10.62 xiP=0.01544 xiPbar=0.001904
Run: 202771 Event: 18236977
 Electron 1: (Q)Pt=(-1)7.532 Et=8.192 det eta=0.1948 eta=0.2489 phi=2.985
 Electron 2: (Q)Pt=(1e+06)1e+06 Et=7.509 det eta=-1.264 eta=-1.216 phi=6.102
 dphi=3.117 angle=2.355 mass=20.13 xiP=0.006496 xiPbar=0.01619
Run: 203153 Event: 12396961
 Electron 1: (Q)Pt=(1)5.578 Et=6.819 det eta=1.478 eta=1.488 phi=0.8746
 Electron 2: (Q)Pt=(-1)6.813 Et=6.407 det eta=0.08953 eta=0.1008 phi=4.011
 dphi=3.137 angle=1.867 mass=16.44 xiP=0.01902 xiPbar=0.003741
Run: 204119 Event: 2569312
 Electron 1: (Q)Pt=(1)4.609 Et=6.049 det eta=-0.4183 eta=-0.4183 phi=3.021
 Electron 2: (Q)Pt=(-1)3.951 Et=5.033 det eta=-0.8484 eta=-1.049 phi=6.161
 dphi=3.141 angle=1.641 mass=11.23 xiP=0.002931 xiPbar=0.01202
Run: 204444 Event: 7996099
 Electron 1: (Q)Pt=(1)14.32 Et=13.81 det eta=0.06527 eta=0.04751 phi=1.648
 Electron 2: (Q)Pt=(1e+06)1e+06 Et=13.25 det eta=0.6749 eta=0.6604 phi=4.782
 dphi=3.133 angle=2.446 mass=28.46 xiP=0.02047 xiPbar=0.01021
Run: 204478 Event: 639495
 Electron 1: (Q)Pt=(1e+06)1e+06 Et=39.75 det eta=0.8918 eta=0.8918 phi=5.441
 Electron 2: (Q)Pt=(1e+06)1e+06 Et=6.095 det eta=-0.7692 eta=-0.7692 phi=1.175
 dphi=2.017 angle=2.316 mass=38.54 xiP=0.05091 xiPbar=0.01502
Run: 205894 Event: 1786515
 Electron 1: (Q)Pt=(-1)11.8 Et=12.67 det eta=0.6686 eta=0.6538 phi=2.155
 Electron 2: (Q)Pt=(1)11.71 Et=11.22 det eta=-0.9574 eta=-0.9696 phi=5.3
 dphi=3.138 angle=2.916 mass=31.94 xiP=0.0146 xiPbar=0.01846
Run: 205894 Event: 7348357
 Electron 1: (Q)Pt=(1)5.67 Et=5.889 det eta=0.3319 eta=-0.2186 phi=2.23
 Electron 2: (Q)Pt=(1e+06)1e+06 Et=5.302 det eta=-1.849 eta=-2.278 phi=5.352
 dphi=3.122 angle=1.605 mass=17.81 xiP=0.002692 xiPbar=0.03014
Run: 205563 Event: 37482
 Electron 1: (Q)Pt=(1)6.811 Et=6.746 det eta=1.156 eta=1.265 phi=2.867
 Electron 2: (Q)Pt=(-1)6.08 Et=6.338 det eta=1.356 eta=1.471 phi=5.996
 dphi=3.129 angle=1.005 mass=13.12 xiP=0.02627 xiPbar=0.001714
Run: 206537 Event: 12488672
 Electron 1: (Q)Pt=(-1)3.143 Et=15.52 det eta=0.5568 eta=0.5568 phi=1.848
 Electron 2: (Q)Pt=(1e+06)1e+06 Et=12.58 det eta=-1.849 eta=-1.849 phi=5.017
 dphi=3.114 angle=2.441 mass=51.89 xiP=0.01483 xiPbar=0.04534
```

7.4 Appendix: Effective Luminosity Calculation

It was shown in Section 4.4 that:

$$\varepsilon_{exc}(\mathscr{L}) = \frac{N_O(\mathscr{L})}{N_T(\mathscr{L})} \tag{21}$$

Where $N_O(\mathscr{L})$ is the number of crossing in which an exclusive interaction can be observed in the dataset in the instantaneous luminosity bin $\mathscr{L}$, and $N_T(\mathscr{L})$ is the number of crossings in the dataset in the instantaneouos luminosity bin $\mathscr{L}$(note that $N_O(\mathscr{L})/N_T(\mathscr{L}) = N_{ZB}^{pass}(\mathscr{L})/N_{ZB}^{total}(\mathscr{L})$.

The total number of crossing in which an exclusive interaction can be observed in the dataset N_O, and the total number of crossings in the dataset N_T, can be written as (the proportionality is just some cross section):

$$N_O \propto \int \varepsilon_{exc} \cdot \mathscr{L}\ dt \tag{22}$$

$$N_T \propto \int \mathscr{L}\ dt \tag{23}$$

They can also be written as an integral over the instantaneous luminosity, $\mathscr{L}$:

$$N_O \propto \int \varepsilon_{exc} \cdot N_T(\mathscr{L}) \cdot \mathscr{L}\ d\mathscr{L} \tag{24}$$

$$N_T \propto \int N_T(\mathscr{L}) \cdot \mathscr{L}\ d\mathscr{L} \tag{25}$$

Taking the ratio of N_O to N_T, with equations 23 and 25, one gets:

$$\frac{N_O}{N_T} = \frac{\int \varepsilon_{exc} \cdot \mathscr{L}\ dt}{\int \mathscr{L}\ dt} = \frac{\int \varepsilon_{exc} \cdot N_T(\mathscr{L}) \cdot \mathscr{L}\ d\mathscr{L}}{\int N_T(\mathscr{L}) \cdot \mathscr{L}\ d\mathscr{L}} \tag{26}$$

Therefore:

$$\mathscr{L}_{eff} \equiv \int \varepsilon_{exc} \mathscr{L} dt = \frac{\int \varepsilon_{exc} \cdot N_T(\mathscr{L}) \cdot \mathscr{L}\ d\mathscr{L}}{\int N_T(\mathscr{L}) \cdot \mathscr{L}\ d\mathscr{L}} \int \mathscr{L} dt \tag{27}$$

References

[1] **W.Bartel et al. (JADE) DESY 86-005. At PETRA, Double tagged e^+e^- and $\mu^+\mu^-$ with $M_{ll} < 1$ GeV.**

[2] **H.Hayashii et al. (TOPAZ) Phys.Lett.B279 (1992) 422. Tagged $\mu^+\mu^-$ At TRISTAN $\sqrt{s} = 52$-61.4 GeV, single tagged $M_{\mu\mu}$ up to ≈ 20 GeV, 3 double tagged events.**

[3] **P.Abreu et al.(DELPHI), hep-ex/0105084 Zeit. fur Phys C XX ($e^+e^- \to e^+e^-\mu^+\mu^-$); J.Abdallah et al., Eur.Phys.J C35 (2004) 159, hep-ex/0406010.**

[4] **R.Akers et al. (OPAL), Z.Phys C60 (1993) 593 ($\mu^+\mu^-$ and $\tau^+\tau^-$); G.Abbiendi et al., Eur.Phys.J C11 (1999) 409.**

[5] **(L3) M.Acciarri et al., Phys.Lett B407 (1997) 341 (untagged $e^+e^-, \mu^+\mu^-, \tau^+\tau^-$); M.Acciarri et al., Phys.Lett.B438 (1998) 363 ; P.Achard et al., Phys.Lett.B585 (2004) 53 (hep-ex/0402037.**

[6] **M.R.Whalley, J.Phys.G: Nucl.Part.Phys. 27 (2001) A1-A121. This is a review only of $e^+e^- \to$ hadrons.**

[7] **J.Vermaseren, Nucl. Phys. B229 (1983) 347-371**

[8] **V.M.Budnev, I.F.Ginsburg, G.V.Meledin and V.G.Serbo, Phys.Lett. 39B (1972) 526.**

[9] **A.G.Shamov and V.I.Telnov, hep-ex/0207095 Nucl.Instrum.Meth. A494 51 (2002)**

[10] **K.Piotrzkowski, hep-ex/0009065, Phys.Rev D63: 071052 (2001)**

[11] **B.L.Caron and J.Pinfold, Helsinki 2000, Workshop on Forward Physics and Luminosity Determination at the LHC.**

[12] **A. Bhatti, Jet Energy Corrections at CDF, CDFNOTE 7543, 2005**

[13] **S. Dube, Low Et electron ID efficiency and scale-factors using J/Psi, CDFNOTE 7379, 2005**

[14] **A. Hamilton, Estimating Effective Luminosity in Rapidity Gap Physics, CDFNOTE 7556, 2005**

[15] **A. Attal, ID Efficiencies for Medium E_T Plug Electrons, CDFNOTE 7345, 2005**

[16] **A.Hamilton et al., First Evidence of Exclusive Photon Pairs in Hadron-Hadron Collisions, CDF/DOC/JET/CDFR/7931**

[17] **G.P. Lepage, J. Comp. Phys. 27 (1978) 192**